
Control, Transport and Sampling: Towards Better Loss Design

Qijia Jiang
UC Davis

David Nabergoj
University of Ljubljana

Abstract

Leveraging connections between diffusion-based sampling, optimal transport, and stochastic optimal control through their shared links to the Schrödinger bridge problem, we propose novel objective functions that can be used to transport ν to μ , consequently sample from the target μ , via *optimally controlled* dynamics. We highlight the importance of the pathwise perspective and the role various optimality conditions on the path measure can play for the design of valid training losses, the careful choice of which offer numerical advantages in implementation. Basing the formalism on Schrödinger bridge comes with the additional practical capability of baking in inductive bias when it comes to Neural Network training.

1 INTRODUCTION

Traditionally, the task of sampling from un-normalized densities is largely delegated to MCMC methods. However, modern machine learning developments in optimal transport and generative modeling have greatly expanded the toolbox we have available for performing such tasks, which can further benefit from powerful advancements in deep learning. By reducing the problem to performing empirical risk minimization with neural networks, they hold promise especially for sampling from high-dimensional and multimodal distributions compared to MCMC-based alternatives. In this work, we propose novel training objectives that are amenable to tractable approximations for sampling (without access to data from the target, as typically considered in the MCMC setup), and demonstrate their numerical advantages compared to several

related methods that are also built around forward-backward SDEs through time-reversals. Before elaborating on these connections and synthesis in Section 2, we briefly summarize our contributions below.

- We present a transport/control based sampler using Schrödinger bridge (SB) idea (generalizable to extended state space and nonlinear prior), which compared to MCMC-based approaches has two benefits: (1) alleviate metastability without being confined to local moves in the state space; (2) based on interpolating path, it comes with the ability to provide low-variance, unbiased normalizing constant estimates using the trajectory information (c.f. Section 3.2).
- Unlike previously studied Schrödinger-bridge-based (Chen et al., 2021a) and diffusion-based samplers (Berner et al., 2022; Vargas et al., 2022; Richter et al., 2023), we explicitly enforce *optimality* and *uniqueness* of the trajectory, which also ensure that the dynamics reaches target in *finite* time. Compared to IPF-based approaches for solving SB (Vargas and Nüsken, 2023), our joint training approach of the forward and backward controls is not susceptible to prior forgetting, at the same time amenable to importance sampling correction for bias coming from neural network training (e.g., approximation error). The algorithm and setup we consider deviates from the more well-studied generative model use case of SB (De Bortoli et al., 2021; Peluchetti, 2023; Shi et al., 2023).
- In contrast to previously proposed losses that follow optimal trajectory for sampling from the target (Vargas and Nüsken, 2023; Liu et al., 2022), our (discretized) training objectives have the numerical advantage of (1) vanishing variance of the stochastic gradient at the optimal control; (2) expense the need for evaluating expensive Laplacian terms. These heavily rely on the path measure based representations of our losses and estimators and generalize much beyond the half bridge case considered in (Zhang and Chen, 2021). Compar-

isons of the performance are given in Section 4 w.r.t alternative loss proposals.

- From a practical standpoint, our SB-based path-wise sampler is both gradient free, and comes with structure in its solution such that special NN architecture can be exploited for training. While we focus our attention on using the SB formalism for sampling, the same methodology can be used for e.g., optimal transport applications.

2 GENERAL FRAMEWORK

In this section we put several recently proposed (and diffusion-related) methods in context, rendering them as special instantiations of a more unifying *path-wise* picture, which will in turn motivate the need for a control-based approach that involves designing an optimal path exactly interpolating between two distributions. We loosely follow the framework put forth in (Vargas and Nüsken, 2023) for parts of the exposition.

2.1 Setup

We are interested in sampling from $p_{\text{target}}(x) = \mu(x)/Z$ by minimizing certain tractable loss, assuming sampling from $p_{\text{prior}}(z) = \nu(z)$ is easy, but unlike in generative modeling, even though analytical expression for μ is readily available, we do not have access to data from it that can be used to learn the score function. In this sense, in terms of “transport mapping”, the two sides are crucially not symmetric. Below we introduce forward-backward SDEs for formalizing such transitions. Pictorially, given a base drift f , we have the “sampling process” (the two processes are time reversals of each other):

$$\nu(z) \begin{array}{c} \xrightarrow{\mathbb{P}^{\nu, f + \sigma u}} \\ \xleftarrow{\mathbb{P}^{\mu, f + \sigma v}} \end{array} \mu(x) \quad (1)$$

for tunable controls u, v and terminal marginals ν, μ . Written as SDEs, they become (the drifts u, v here are not independent)

$$\begin{aligned} dX_t &= [f_t(X_t) + \sigma u_t(X_t)]dt + \sigma d\overrightarrow{W}_t, \quad X_0 \sim \nu \quad (2) \\ &\Rightarrow (X_t)_{t \in [0, T]} \sim \overrightarrow{\mathbb{P}}^{\nu, f + \sigma u}, \end{aligned}$$

$$\begin{aligned} dX_t &= [f_t(X_t) + \sigma v_t(X_t)]dt + \sigma d\overleftarrow{W}_t, \quad X_T \sim \mu \quad (3) \\ &\Rightarrow (X_t)_{t \in [0, T]} \sim \overleftarrow{\mathbb{P}}^{\mu, f + \sigma v}. \end{aligned}$$

Operationally, (2)-(3) denote (picking $f = 0$, and $\{z_t\}$ a sequence of i.i.d standard Gaussians for illustration)

$$\begin{aligned} X_t &= X_0 + \int_0^t \sigma u_s(X_s)ds + \int_0^t \sigma d\overrightarrow{W}_s \\ &\Rightarrow X_{t+h} \approx X_t + h\sigma u_t(X_t) + \sqrt{h}\sigma z_t, \quad X_0 \sim \nu \end{aligned}$$

$$\begin{aligned} X_t &= X_T - \int_t^T \sigma v_s(X_s)ds - \int_t^T \sigma d\overleftarrow{W}_s \\ &\Rightarrow X_{t-h} \approx X_t - h\sigma v_t(X_t) + \sqrt{h}\sigma z_t, \quad X_T \sim \mu \end{aligned}$$

where the forward (the usual Itô’s) and the backward integrals indicate different endpoints at which we make the approximation. For processes $(Y_t)_t, (Z_t)_t$,

$$\int_0^T a_t(Y_t) d\overrightarrow{Z}_t \approx \sum_i a_{t_i}(Y_{t_i})(Z_{t_{i+1}} - Z_{t_i}), \quad (4)$$

$$\int_0^T a_t(Y_t) d\overleftarrow{Z}_t \approx \sum_i a_{t_{i+1}}(Y_{t_{i+1}})(Z_{t_{i+1}} - Z_{t_i}), \quad (5)$$

which in particular implies the martingale property

$$\mathbb{E}_{X \sim \overrightarrow{\mathbb{P}}^{\nu, f + \sigma u}} \left[\int_0^t a_s(X_s) d\overrightarrow{W}_s \right] = 0, \quad (6)$$

$$\mathbb{E}_{X \sim \overleftarrow{\mathbb{P}}^{\mu, f + \sigma v}} \left[\int_{T-t}^T a_s(X_s) d\overleftarrow{W}_s \right] = 0. \quad (7)$$

Forward/backward integral can be converted through

$$\sigma^2 \int_0^T (\nabla \cdot a_t)(Y_t) dt + \int_0^T a_t(Y_t) d\overrightarrow{Z}_t = \int_0^T a_t(Y_t) d\overleftarrow{Z}_t, \quad (8)$$

which will be used repeatedly throughout.

Remark 1 (Nelson’s identity). The following relationship between drifts for the SDE (2)-(3) is well known: $\overrightarrow{\mathbb{P}}^{\nu, f + \sigma u} = \overleftarrow{\mathbb{P}}^{\mu, f + \sigma v}$ iff $\overrightarrow{\mathbb{P}}_T^{\nu, f + \sigma u} = \mu$, and $\sigma v_t(X_t) = \sigma u_t(X_t) - \sigma^2 \nabla \log(\overrightarrow{\mathbb{P}}_t^{\nu, f + \sigma u}) = \sigma u_t(X_t) - \sigma^2 \nabla \log(\overleftarrow{\mathbb{P}}_t^{\mu, f + \sigma v})$ for all $t \in [0, T]$. This is used to give a more transparent derivation of the likelihood ratio in Lemma 3.

2.2 Goal and Related Approaches

Forward KL We would like the two path measures (with the specified two end-point marginals) to agree progressing in either direction. The methods in (Vargas et al., 2022; Zhang and Chen, 2021) propose to set up a reference process with a similar structure as (1) with $f = 0$:

$$\nu(z) \begin{array}{c} \xrightarrow{\mathbb{P}^{\nu, \sigma r}} \\ \xleftarrow{\mathbb{P}^{\eta, \sigma v}} \end{array} \eta(x) \quad (9)$$

where r is the drift for a reference process:

$$dX_t = \sigma r_t(X_t) dt + \sigma d\overrightarrow{W}_t, \quad X_0 \sim \nu \Rightarrow (X_t)_{t \in [0, T]} \sim \overrightarrow{\mathbb{P}}^{\nu, \sigma r} \quad (10)$$

and $\eta = \overrightarrow{\mathbb{P}}_T^{\nu, \sigma r}$. Via Girsanov’s theorem, the method amounts to minimizing loss of the following type: $\mathcal{L}_{KL}(u) =$

$$\mathbb{E}_{\overrightarrow{\mathbb{P}}^{\nu, \sigma u}} \left[\log \left(\frac{d\overrightarrow{\mathbb{P}}^{\nu, \sigma u}}{d\overrightarrow{\mathbb{P}}^{\mu, \sigma v}} \right) \right] = \mathbb{E}_{\overrightarrow{\mathbb{P}}^{\nu, \sigma u}} \left[\log \left(\frac{d\overrightarrow{\mathbb{P}}^{\nu, \sigma u}}{d\overrightarrow{\mathbb{P}}^{\nu, \sigma r}} \frac{d\overleftarrow{\mathbb{P}}^{\eta, \sigma v}}{d\overleftarrow{\mathbb{P}}^{\mu, \sigma v}} \right) \right]$$

$$\begin{aligned}
 &= \mathbb{E}_{\overleftarrow{\mathbb{P}}^{\nu, \sigma u}} \left[\log \left(\frac{d\overleftarrow{\mathbb{P}}^{\nu, \sigma u}}{d\overleftarrow{\mathbb{P}}^{\nu, \sigma r}} \frac{d\eta}{d\mu} \right) + \log Z \right] \\
 &= \mathbb{E}_{X \sim \overleftarrow{\mathbb{P}}^{\nu, \sigma u}} \left[\int_0^T \frac{1}{2} \|u_s(X_s) - r_s(X_s)\|^2 ds + \log \left(\frac{d\eta}{d\mu} \right) (X_T) \right] \\
 &\quad + \log Z. \tag{11}
 \end{aligned}$$

This suggests initializing from ν to estimate the loss (11) with the current control $u^\hat{\theta}$ by simulating (2), followed by gradient descent to optimize the $\hat{\theta}$ -parameterized control and iterating between the two steps can be a viable strategy, that could identify u^{θ^*} eventually and used to run (2) to draw samples from μ . Note η, ν are simple distributions we have the freedom to pick, along with $r(\cdot)$ in (9). The judicious choice of the common v and ν in (1) and (9) allow (11) to take on a control-theoretic interpretation (Berner et al., 2022), where the cost (11) is composed of a running control cost and a terminal cost.

For a concrete example consider $\nu = \mathcal{N}(0, \sigma^2 I)$, $r_t(x) = -x/2\sigma$ in (10), then process (9) is simply OU in equilibrium, i.e., $\nu = \eta$ (Vargas et al., 2022). The purpose of introducing the reference process (9) is to fix the backward drift v in (1) so that $\min_u \mathcal{L}_{KL}(u)$ from (11) is unique. However, this example illustrates that in general unless $T \rightarrow \infty$, $\mathcal{L}_{KL}(u)$ in (11) can't be minimized to 0 since $\overleftarrow{\mathbb{P}}_0^{\mu, \sigma v} \neq \nu$ under the OU process with $v_t(x) = x/2\sigma$ unless $T \rightarrow \infty$.

Remark 2. The loss (11) enforces uniqueness (and correct marginals ν, μ) if minimized to 0, but doesn't impose optimality of the interpolating trajectory in any way. The approach in (Chen et al., 2021a) that relies on training two drifts amounts to solving $\min_{u, v} D_{KL}(\overleftarrow{\mathbb{P}}^{\nu, f+\sigma u} \| \overleftarrow{\mathbb{P}}^{\mu, f+\sigma v})$ jointly, and as shown in (Richter et al., 2023), although ensure correct marginals, has non-unique minimizers. A unique solution is desirable since it ensures robustness - one gets the same marginal density trajectory regardless of the initialization/training procedure.

Reverse KL In diffusion generative modeling, score-matching-based loss (Hyvärinen and Dayan, 2005) can be seen as minimizing the reverse KL over $s := (u - v)/\sigma$ by running the backward process (3) using samples from μ to estimate the loss. More concretely, using the Radon-Nikodym derivative in Lemma 3, it gives $\mathcal{L}_{KL}(s) =$

$$\begin{aligned}
 &\mathbb{E}_{\overleftarrow{\mathbb{P}}^{\mu, \sigma v}} \left[\log \left(\frac{d\overleftarrow{\mathbb{P}}^{\mu, \sigma v}}{d\overleftarrow{\mathbb{P}}^{\nu, \sigma u}} \right) \right] = \mathbb{E}_{\overleftarrow{\mathbb{P}}^{\mu, \sigma v}} \left[\log \left(\frac{d\overleftarrow{\mathbb{P}}^{\mu, \sigma v}}{d\overleftarrow{\mathbb{P}}^{\nu, \sigma v + \sigma^2 s}} \right) \right] = \\
 &\mathbb{E}_{\overleftarrow{\mathbb{P}}^{\mu, \sigma v}} \left[\int_0^T \frac{\sigma^2}{2} \|s_t(X_t)\|^2 dt + \sigma^2 \int_0^T \nabla \cdot s_t(X_t) dt \right] + C = \\
 &\mathbb{E}_{\overleftarrow{\mathbb{P}}^{\mu, \sigma v}} \left[\int_0^T \frac{\sigma^2}{2} \|s_t(X_t) - \nabla_x \log p_t^{\mu, \sigma v}(X_t | X_T = x_T)\|^2 dt \right] \\
 &\quad + C'. \tag{12}
 \end{aligned}$$

where C, C' is independent of s . Here one fixes the backward drift v in $\overleftarrow{\mathbb{P}}^{\mu, \sigma v}$ so that ν is easy to sample from (e.g., an OU process). In the last transition above, we used the integration by parts identity $\mathbb{E}_{\rho_t} [\int_0^T s_t^\top \nabla \log \rho_t dt] = -\mathbb{E}_{\rho_t} [\int_0^T \nabla \cdot s_t dt]$. In practice crucially there will be an irreducible loss since the terminals ν and $\overleftarrow{\mathbb{P}}_0^{\mu, \sigma v}$ don't match exactly for any finite T , but the dynamics $\overleftarrow{\mathbb{P}}^{\nu, \sigma v + \sigma^2 s}$ still makes sense as for two processes $(p_t)_t, (q_t)_t$ with different initializations $\nu, \overleftarrow{\mathbb{P}}_0^{\mu, \sigma v}$ that share the same drift $\sigma v + \sigma^2 s^*$, $\partial_t D_{KL}(p_t \| q_t) = -\mathbb{E}_{p_t} [\|\nabla \log \frac{p_t}{q_t}\|^2] \leq 0$ contracts (c.f. Remark 16), although we have not been quantitative about the rate. It is worth noting that such approach doesn't require re-generating trajectories iteratively as (11) does.

We therefore see that both the approach of (11) and (12) rely on fixing some aspect of the process in (1) to restore uniqueness of the loss \mathcal{L}_{KL} , but this choice is mostly out of convenience. In both cases, it results in an *one-parameter loss*, and the minimizer is not affected by the unknown constant Z . Successfully optimizing $D_{KL}(\overleftarrow{\mathbb{P}}^{\nu, \sigma u} \| \overleftarrow{\mathbb{P}}^{\mu, \sigma v})$ or $D_{KL}(\overleftarrow{\mathbb{P}}^{\mu, \sigma v} \| \overleftarrow{\mathbb{P}}^{\nu, \sigma u})$ to zero error will imply that u pushes ν to μ and v vice versa, mimicking a noising/denoising reversible procedure. In what follows in Section 3, we deviate from these perspectives by adopting a control formulation that does not rely on mixing of stochastic processes for transporting between two distributions, albeit still working with a pathwise formulation.

3 METHODOLOGY

As we saw from Section 2, (1) relying on mixing property of diffusion process can make the trajectory rather long; (2) there are many degrees of freedom in transporting ν to μ , neither of which is desirable for training purpose. This gives us the motivation to turn to losses based on path measures that can enforce a canonical choice (c.f. Appendix A for additional practical motivation behind SB vs. other pathwise samplers). We will adopt an "optimal control" perspective and leverage special properties of the SB problem to come up with valid control objectives for this effort. Consider over path space $\mathcal{C}([0, T]; \mathbb{R}^d)$, given a reference measure Q , the *constrained* optimization problem

$$P^* = \arg \min_{P_0=\nu, P_T=\mu} D_{KL}(P \| Q) \tag{13}$$

where we assume Q admits the SDE representation (this can be thought of as a prior)

$$dX_t = f_t(X_t) dt + \sigma dW_t, \quad X_0 \sim \nu, \tag{14}$$

which is a slight generalization of the classical case where typically $f = 0$. Furthermore the path measure

P is assumed to correspond to the following SDE and we are interested in finding the optimal control ϕ in

$$dX_t = [f_t(X_t) + \sigma^2 \nabla \phi_t(X_t)] dt + \sigma dW_t, \quad X_0 \sim \nu \quad (15)$$

that solves (13). Various perspectives on the Schrödinger Bridge problem (13)-(14), which we heavily leverage in the next part for designing our losses, are included in Appendix B, along with related methods for solving the problem in different setups than what we consider in Appendix C.

3.1 Training Loss Proposal

Recall our focus is on solving the regularized optimal transport problem (13) between ν and μ , by learning the controls on the basis of samples from ν . Out

of many joint couplings with correct marginals (i.e., transport maps), the choice of a reference process will select a particular trajectory ρ_t between ν and μ . The execution of this plan crucially hinges on two ingredients: (1) general backward / forward likelihood ratio formula given in Lemma 3; (2) properties of the optimal drifts for SB from Section B, some of which can be exploited for training the controls. Challenge, as emphasized before, is we need to be able to estimate the resulting loss and ensuring that successful optimization guarantees convergence to the unique solution dictated by the SB. Proposition 1 below serves as our main result, where we show that adding appropriate regularization can accomplish these. All proofs are deferred to Appendix D.

Proposition 1 (Control Training Objective). *For the problem of (13), the following losses are valid:*

$$(a) \arg \min_{\nabla \phi, \nabla \psi} D_{KL}(\overrightarrow{\mathbb{P}}^{\nu, f + \sigma^2 \nabla \phi} \parallel \overleftarrow{\mathbb{P}}^{\mu, f - \sigma^2 \nabla \psi}) + \lambda \cdot \mathbb{E}_{X \sim \overrightarrow{\mathbb{P}}^{\nu, f + \sigma^2 \nabla \phi}} \left[\int_0^T \frac{\sigma^2}{2} \|\nabla \phi_t(X_t)\|^2 dt \right]$$

$$(b) \arg \min_{\nabla \phi, \nabla \psi} \text{Var}_{\overrightarrow{\mathbb{P}}^{\nu, f + \sigma^2 \nabla \phi}} \left[\log \left(\frac{\overrightarrow{\mathbb{P}}^{\nu, f + \sigma^2 \nabla \phi}}{\overleftarrow{\mathbb{P}}^{\mu, f - \sigma^2 \nabla \psi}} \right) \right] +$$

$$\text{Var}_{X \sim \overrightarrow{\mathbb{P}}^{\nu, f}} \left(\psi_T(X_T) - \psi_0(X_0) + \int_0^T \left(-\frac{\sigma^2}{2} \|\nabla \psi_t\|^2 + \nabla \cdot f_t - \sigma^2 \Delta \psi_t \right) (X_t) dt - \sigma \int_0^T \nabla \psi_t(X_t)^\top dW_t \right)$$

$$\text{or } \text{Var}_{X \sim \overrightarrow{\mathbb{P}}^{\nu, f}} \left(\phi_T(X_T) - \phi_0(X_0) + \frac{\sigma^2}{2} \int_0^T \|\nabla \phi_t\|^2(X_t) dt - \sigma \int_0^T \nabla \phi_t(X_t)^\top dW_t \right)$$

$$(c) \arg \min_{\phi, \psi} \text{Var}_{X \sim \overrightarrow{\mathbb{P}}^{\nu, f + \sigma^2 \nabla \phi}} ((\phi_T + \psi_T - \log \mu)(X_T)) + \text{Var}_{X \sim \overrightarrow{\mathbb{P}}^{\nu, f + \sigma^2 \nabla \phi}} ((\phi_0 + \psi_0 - \log \nu)(X_0)) +$$

$$\text{Var}_{X \sim \overrightarrow{\mathbb{P}}^{\nu, f + \sigma^2 \nabla \phi}} \left(\phi_T(X_T) - \phi_0(X_0) - \frac{\sigma^2}{2} \int_0^T \|\nabla \phi_t\|^2(X_t) dt - \sigma \int_0^T \nabla \phi_t(X_t)^\top dW_t \right) +$$

$$\text{Var}_{X \sim \overrightarrow{\mathbb{P}}^{\nu, f + \sigma^2 \nabla \phi}} \left(\psi_T(X_T) - \psi_0(X_0) - \int_0^T \left(\frac{\sigma^2}{2} \|\nabla \psi_t\|^2 + \nabla \cdot (\sigma^2 \nabla \psi_t - f_t) + \sigma^2 \nabla \psi_t^\top \nabla \phi_t \right) (X_t) dt - \sigma \int_0^T \nabla \psi_t(X_t)^\top dW_t \right)$$

$$(d) \arg \min_{\nabla \phi_t, \nabla \log \rho_t} D_{KL}(\overrightarrow{\mathbb{P}}^{\nu, f + \sigma^2 \nabla \phi_t} \parallel \overleftarrow{\mathbb{P}}^{\mu, f + \sigma^2 \nabla \phi_t - \sigma^2 \nabla \log \rho_t}) + \lambda \cdot \mathbb{E}_{\overrightarrow{\mathbb{P}}^{\nu, f + \sigma^2 \nabla \phi}} \left[\int_0^T \frac{\sigma^2}{2} \|\nabla \phi_t(X_t)\|^2 dt \right]$$

In particular, if the loss is minimized to 0 for (b) and (c), the resulting $\nabla \phi^*$ solves the SB problem (13) from ν to μ , that can in turn be used for sampling from μ by running (15). In all cases, $X_0 = x_0 \sim \nu$ is assumed given as initial condition. Moreover, $\nabla \psi^*$ is the corresponding backward drift that drives μ to ν .

Both (a) and (d) are guided by the “minimum-action” principle w.r.t a reference (i.e., minimum control energy spent). (b) bases itself on a reformulation of the HJB PDE involving the optimal control, and (c) is grounded in the FBSDE system for SB optimality (Chen et al., 2021a) (c.f. Remark 13 for connections between particular SDEs, PDEs and path measures). In all cases, the objective is a *two-parameter loss* that also allows the recovery of the score $\nabla \log \rho_t$. Note that variance is taken w.r.t the uncontrolled process in (b) and w.r.t the controlled process in (c). Losses (a) and (d), being conversion from the constrained problem (and each other), need λ to be picked relatively small

so that the first part of the objective = 0 to identify the unique SB solution, but we establish a bound on the optimal objective value in Remark 7. The proof of these results heavily use the factorization property (47) satisfied by the optimal coupling, and exploit different ways to encode the optimality condition.

Loss (c) is different from log-variance divergence over path space $\text{Var}_{\overrightarrow{\mathbb{P}}^{\nu, f + \sigma^2 \nabla \phi}} \left[\log \left(\frac{d\overrightarrow{\mathbb{P}}^{\nu, f + \sigma^2 \nabla \phi}}{d\overleftarrow{\mathbb{P}}^{\mu, f - \sigma^2 \nabla \psi}} \right) \right]$, which will *not* guarantee finding the optimal path, whereas the objective in (c) incorporates the dynamics of *two* controlled (and coupled) dynamics w.r.t $\overrightarrow{\mathbb{P}}^{\nu, f}$ that we know how to characterize optimality for using results

in Section B. More specifically, we *separately* impose optimality condition on

$$\log \left(\frac{d\overrightarrow{\mathbb{P}}^{\nu, f + \sigma^2 \nabla \phi_t}}{d\overrightarrow{\mathbb{P}}^{\nu, f}} \right) (X) \text{ and } \log \left(\frac{d\overrightarrow{\mathbb{P}}^{\nu, f}}{d\overleftarrow{\mathbb{P}}^{\mu, f - \sigma^2 \nabla \psi_t}} \right) (X) \quad (16)$$

for $X \sim \overrightarrow{\mathbb{P}}^{\nu, f + \sigma^2 \nabla \phi_t}$ to take factorized forms, as opposed to looking at divergence metrics on their sum $\log \left(\frac{d\overrightarrow{\mathbb{P}}^{\nu, f + \sigma^2 \nabla \phi}}{d\overleftarrow{\mathbb{P}}^{\mu, f - \sigma^2 \nabla \psi}} \right)$ only, effectively erasing the ‘‘SB optimality enforcement’’ part. Another way to view the variance regularizers in loss (b) and (c) is through the SDE representation of the controls from Lemma 4 and observe that the variance condition precisely encodes the optimally-controlled dynamical information. It is important to note that we are evaluating the change of ϕ, ψ on a particular stochastic trajectory, rather than tracking the cumbersome evolution of density over the full \mathbb{R}^d space, as what the PDEs (41) may suggest.

Remark 3 (Stochastic gradient w.r.t controls at optimality). In (Richter et al., 2023), the authors show that log-variance divergence has the advantage of having variance of gradient = 0 at the optimal ϕ^*, ψ^* , which is not true for D_{KL} in general, and has consequence for gradient-based updates such as those in Algorithm 1. Similar argument applies to the variance regularizer we consider (e.g., loss (b)). For this, we look at the Gâteaux derivative of the variance function V in an arbitrary direction τ since from the chain rule $\frac{\delta}{\delta \phi} V(\phi, \psi; \tau) := \frac{d}{d\epsilon} |_{\epsilon=0} V(\phi + \epsilon \tau, \psi) \Rightarrow \partial_{\theta_i} V(\phi_\theta, \psi_\gamma) = \frac{\delta}{\delta \phi} |_{\phi=\phi_\theta} V(\phi, \psi_\gamma; \partial_{\theta_i} \phi_\theta)$. Now if \hat{V} is the Monte-Carlo estimate of the variance of a random quantity $g(\cdot)$, it is always the case that (we use $\frac{\delta}{\delta \phi}(\cdot)_\tau$ to denote derivative in the τ direction)

$$\begin{aligned} \frac{\delta}{\delta \phi} \hat{V}(\phi, \psi; \tau) &= \frac{\delta}{\delta \phi} (\hat{\mathbb{E}}[g(\phi, \psi)^2] - \hat{\mathbb{E}}[g(\phi, \psi)]^2)_\tau \\ &= 2\hat{\mathbb{E}}[g(\phi, \psi) \frac{\delta}{\delta \phi} g(\phi, \psi)_\tau] - 2\hat{\mathbb{E}}[g(\phi, \psi)] \frac{\delta}{\delta \phi} \hat{\mathbb{E}}[g(\phi, \psi)]_\tau. \end{aligned}$$

Hence if $g(\phi^*, \psi^*) = \text{const}$ a.s. for every i.i.d sample, such as the regularizer in loss (b), the derivative w.r.t the control ϕ in direction $\partial_{\theta_i} \phi_\theta$ is 0 at optimality, implying $\text{Var}(\partial_{\theta_i} \hat{V}(\phi_{\theta^*}, \psi_{\gamma^*})) = 0$ by the chain rule.

It’s natural to ask if one can replace the variance regularizer $\text{Var}(\cdot)$ with a moment regularizer $\mathbb{E}[|\cdot|^2]$ in e.g., loss (c). However while the variance is oblivious to constant shift, the moment loss will require knowledge of the normalizing constant Z of the target μ to make sense. In the case of loss (b), using the martingale property (6) and Lemma 4, an alternative proposal based on moment regularizer for e.g., ϕ can be

$$\mathbb{E}_{X \sim \overrightarrow{\mathbb{P}}^{\nu, f}} \left[\underbrace{\left| \phi_T(X_T) - \phi_0(X_0) + \frac{\sigma^2}{2} \int_0^T \|\nabla \phi_t\|^2(X_t) dt \right|^2}_{\bar{g}(\phi)^2} \right].$$

However, the Gâteaux derivative of the loss in this case takes the form of

$$\frac{\delta}{\delta \phi} (\hat{\mathbb{E}}[\bar{g}(\phi)^2])_\tau = 2\hat{\mathbb{E}}[\bar{g}(\phi) \frac{\delta}{\delta \phi} \bar{g}(\phi)_\tau],$$

which means that while $\mathbb{E}[\bar{g}(\cdot)] = 0$ vanish for the optimal control ϕ^* in expectation, for individual trajectory $\bar{g}_i(\cdot) \neq 0$ generally at ϕ^* , hence yielding non-vanishing variance for stochastic gradient and posing challenges for optimization. For our variance regularizer in loss (b) where $g_i(\phi) := \phi_T(X_T^i) - \phi_0(X_0^i) + \frac{\sigma^2}{2} \int_0^T \|\nabla \phi_t\|^2(X_t^i) dt - \sigma \int_0^T \nabla \phi_t(X_t^i)^\top dW_t$ is 0 almost surely for every trajectory at ϕ^* , it implies vanishing gradient and will therefore identify the optimal ϕ^* even with mini-batch updates. In terms of the actual minimum value of the empirical loss, our loss (b) obeys $\hat{V}[g(\phi^*)] = 0$ whereas using Itô’s isometry $\hat{\mathbb{E}}[g(\phi^*)^2] = \hat{\mathbb{E}}[\int \sigma^2 \|\nabla \phi_t^*\|^2 dt] \neq 0$ is much less predictable for monitoring the performance of the final control. This is somewhat similar to (Zhou et al., 2021) where the authors observe that including random 0-mean martingale terms is important for variance reduction in a different context.

Remark 4 (Comparisons). In (Vargas and Nüsken, 2023), the authors propose $\int_0^T \mathbb{E} |\partial_t \phi + f^\top \nabla \phi + \frac{\sigma^2}{2} \Delta \phi + \frac{\sigma^2}{2} \|\nabla \phi\|^2 | (X_t) dt$ as the HJB regularizer (c.f. (33)) on top of $D_{KL}(\overrightarrow{\mathbb{P}}^{\nu, f + \sigma^2 \nabla \phi} \| \overleftarrow{\mathbb{P}}^{\mu, f - \sigma^2 \nabla \psi})$ as the training loss, inspired by PINN (Raissi et al., 2019). As is clear from the proof in Proposition 1, it is equally valid for identifying the optimal drift as our loss (b) (see also related result in (Nüsken and Richter, 2021)). Combining (33)-(34) we can also get a HJB for the backward drift $\nabla \psi$, which read as $\partial_t \psi + f^\top \nabla \psi + \nabla \cdot f - \frac{\sigma^2}{2} \Delta \psi - \frac{\sigma^2}{2} \|\nabla \psi\|^2 = 0$ for imposing the PINN loss. By trading a PDE constraint for a SDE one (based on likelihood ratio of path measures), we can avoid evaluating the divergence term, in addition to the benefit of ‘‘sticking to the landing’’ (c.f. Remark 3). We refer to Section 4 for numerical illustration.

In Appendix F, we consider the extension of such training methodology to the case of second-order dynamics in the augmented (X, V) space à la under-damped Langevin.

3.2 Discretization & Implementation

We discuss implementation of our losses and estimators here. In practice, with imperfect controls from the training procedure, one can perform importance sampling to correct for the bias / improve on the estimate – something only available for path-wise samplers working in extended state space.

Proposition 2 (Importance Sampling). *The follow-*

ing can be used to give unbiased estimate of the normalizing constant for p_{target} :

- (1) For the optimal ϕ^*, ψ^* , with $X_t \sim \overrightarrow{\mathbb{P}}^{\nu, f + \sigma^2 \nabla \phi^*}$,
 $Z = \frac{\mu(X_T)}{\nu(X_0)} \exp\left(\frac{\sigma^2}{2} \int_0^T \nabla \cdot (\nabla \phi_t^* - \nabla \psi_t^*)(X_t) dt + \int_0^T \nabla \cdot f_t(X_t) dt\right)$.
- (2) For any suboptimal ϕ, ψ , with $X_t \sim \overrightarrow{\mathbb{P}}^{\nu, f + \sigma^2 \nabla \phi}$,
 $Z = \mathbb{E}[\exp(-\frac{\sigma^2}{2} \int_0^T \|\nabla \phi_t + \nabla \psi_t\|^2 + \nabla \cdot (f_t - \sigma^2 \nabla \psi_t) dt - \sigma \int_0^T \nabla \phi_t + \nabla \psi_t dW_t - \log \frac{\nu(X_0)}{\mu(X_T)})]$.

With a sub-optimal control $\nabla \phi$ and $X_t \sim \overrightarrow{\mathbb{P}}^{\nu, f + \sigma^2 \nabla \phi}$, re-weighting can be used to get an unbiased estimator of a statistics $g: \mathbb{R}^d \rightarrow \mathbb{R}$ as

$$\frac{\mathbb{E}_\phi[g(X_T)w^\phi(X_T)]}{\mathbb{E}_\phi[w^\phi(X_T)]} = \mathbb{E}_{\phi^*}[g(X_T)] = \mathbb{E}_{p_{\text{target}}}[g]$$

Lemma 1 (Discretized Loss and Estimator). For $X \sim \overrightarrow{\mathbb{P}}^{\nu, f + \sigma^2 \nabla \phi}$, the last part of loss (c) on ψ can be estimated

$$\text{Var}_N\left(\psi_K(X_{K+1}^i) - \psi_0(X_0^i) + \frac{1}{2\sigma^2 h} \sum_{k=0}^{K-1} \|X_{k+1}^i - X_k^i - f_k(X_k^i)h\|^2 - \|X_k^i - X_{k+1}^i + (f_{k+1} - \sigma^2 \nabla \psi_{k+1})(X_{k+1}^i)h\|^2\right),$$

where Var_N denotes empirical estimate of the variance using N samples.

The importance-weighted Z -estimator from Proposition 2 can be approximated as

$$\hat{Z} = \frac{1}{N} \sum_{i=1}^N \exp\left(\log \frac{\mu(X_K^i)}{\nu(X_0^i)} + \frac{1}{2} \sum_{k=0}^{K-1} \|z_k^i\|^2 - \frac{1}{2\sigma^2 h} \|X_k^i - X_{k+1}^i + (f_{k+1} - \sigma^2 \nabla \psi_{k+1})(X_{k+1}^i)h\|^2\right). \quad (17)$$

In both cases for $i \in [N]$ independently, $z_k^i \sim \mathcal{N}(0, I)$, $X_{k+1}^i = X_k^i + (f_k(X_k^i) + \sigma^2 \nabla \phi_k(X_k^i))h + \sigma\sqrt{h} \cdot z_k^i$.

Putting everything together gives the final algorithm.

Algorithm 1 Control Objective Training for Sampling from Un-normalized Density

Require: Initial draw $(X_0^{i,(0)})_{i=1}^N \in \mathbb{R}^d \sim \nu$ independent, initial controls $\phi^{(0)}, \psi^{(0)}$

Require: Un-normalized density μ , base drift f , num of time steps K , num of iterations T

for $t = 0, \dots, T - 1$ **do**

 Run (18) with current control $(\nabla \phi_k^{(t)})_{k=0, \dots, K}$ to obtain $(X_k^{n,(t)})_{k=0, \dots, K}$ for $n = 1, \dots, N$

 Estimate the loss (19) + discretized regularizer (c.f. Lemma 1 & Section 4.1) and the gradient w.r.t the two parameterized controls using the samples $(X_k^{n,(t)})_{k=0, \dots, K, n=1, \dots, N}$

 Gradient update on the parameters to obtain $\nabla \phi^{(t+1)}$ and $\nabla \psi^{(t+1)}$

end for

return $X_K^{1,(T)}, \dots, X_K^{N,(T)}$ as N samples from μ with their importance weights $w^{\phi^{(T)}}(X_K^{n,(T)})$ (92), and the weighted Z estimator (17) for μ

with weight

$$w^\phi(X) = \exp\left(\int_0^T \sigma^2 \Delta \phi_t - \frac{\sigma^2}{2} \Delta \log \rho_t + \nabla \cdot f_t dt\right) \frac{d\mu(X_T^\phi)}{d\nu(X_0^\phi)}.$$

As in (Vargas and Nüsken, 2023, Proposition F.1), it is possible to trade divergence term for a backward integral when dealing with path integrals using (8). Thanks to the fact that our various estimators and regularizers are built upon path measures, the following lemma generalizes this idea and provides a recipe for estimating the regularizer from Proposition 1 and the normalizing constant from Proposition 2 with discrete-time updates that are cheap to evaluate. We work out loss (c) from Proposition 1 below – most other parts are straightforward to adapt so we simply state them in Section 4.1.

We also draw a connection between the optimal Z estimator and the optimal controls below.

Remark 5 (Optimal $\log Z$ estimator). As observed in (Vargas and Nüsken, 2023), discretizations with backward integral have the additional benefit of giving ELBO lower bound for the normalizing constant Z of p_{target} . Since our \hat{Z} -estimator from Lemma 1 can be understood as a ratio of two discrete chains

$$\hat{Z} = \frac{\mu(X_K)q^v(X_{0:K-1}|X_K)}{\nu(X_0)p^u(X_{1:K}|X_0)},$$

it implies that $\mathbb{E}_{\nu(X_0)p^u(X_{1:K}|X_0)}[\log \hat{Z}] \leq \log(\mathbb{E}_{\nu(X_0)p^u(X_{1:K}|X_0)}[\hat{Z}]) = \log[\int \mu(X_K) dX_K] = \log(Z)$. The estimator is reminiscent of the philosophy adopted in annealed importance sampling (AIS) with extended target, but in our case, the backward kernel $q^v(\cdot)$ is the *time-reversal* of the forward one, which can be shown to be the optimal transition kernel minimizing the variance of the resulting evidence estimate (Doucet et al., 2022). In addition, the forward kernel $p^u(\cdot)$ in our case follows an optimal trajectory that ensures the chain reaches the *exact*

target μ rapidly.

4 NUMERICS & COMPARISONS

In this section, we instantiate our main contributions (Proposition 1 and Lemma 1) and offer numerical evidence on their advantages compared to existing proposals for solving an optimal trajectory problem in a typical MCMC setup. We highlight that our algorithm does not use gradient information from the target $\nabla \log \mu$ as e.g., Langevin would.

4.1 Algorithm Specification

Below for simplicity we pick the reference process to be a Brownian motion with $f = 0$ and λ is a parameter that we tune for best performance, but in theory any $\lambda > 0$ would work. This aspect deviates from other constrained formulation of the problem that may require special choice of λ .

(1) PINN-regularization (Vargas and Nüsken, 2023): for $i = 1, \dots, n$, and $Z \sim \mathcal{N}(0, I)$ independently draw in parallel

$$x_{k+1}^i = x_k^i + \sigma^2 h \nabla \phi(x_k^i, kh) + \sigma \sqrt{h} Z_k^i, x_0^i \sim \nu \quad (18)$$

for $k = 0, \dots, K$ with stepsize $h = c/(K+1)$ for some $c \geq 1$. Using trajectories $\{x_k^i\}$, minimize over ϕ, ψ ,

$$\begin{aligned} & \frac{1}{K+1} \text{Var}_n \left[\log \frac{\nu(x_0^i)}{\mu(x_{K+1}^i)} + \right. \\ & \left. \sum_{k=0}^K \frac{1}{2\sigma^2 h} (\|x_k^i - x_{k+1}^i - \sigma^2 h \nabla \psi(x_{k+1}^i, (k+1)h)\|^2 \right. \\ & \left. - \|x_{k+1}^i - x_k^i - \sigma^2 h \nabla \phi(x_k^i, kh)\|^2) \right] + \end{aligned} \quad (19)$$

$$\frac{\lambda h}{n} \sum_{i=1}^n \sum_{k=0}^K \left| \partial_t \phi(x_k^i, kh) + \frac{\sigma^2}{2} \Delta \phi(x_k^i, kh) + \frac{\sigma^2}{2} \|\nabla \phi(x_k^i, kh)\|^2 \right| \quad (20)$$

The first term (19) is an estimate of the log-variance divergence between the two path measures. Above $\phi(x, t), \psi(x, t)$ are two neural networks that take $t \in \mathbb{R}$ and $x \in \mathbb{R}^d$ as inputs and map to \mathbb{R} . We repeat (18) and (20) several times, and compute statistics using samples $\{x_{K+1}^i\}_{i=1}^n$ at the end.

(2) Variance-regularization (loss (b) from Proposition 1): Simulate trajectories (18) as before, additionally simulate $\{y_k^i\}_{k=0}^K$ as follows and cache them:

$$y_{k+1}^i = y_k^i + \sigma \sqrt{h} Z_k^i, y_0^i \sim \nu. \quad (21)$$

Minimize over ϕ, ψ the following discretized loss

$$(19) + \frac{\lambda}{K+1} \cdot \text{Var}_n \left[\phi(y_{K+1}^i, (K+1)h) - \phi(y_0^i, 0) + \frac{1}{2\sigma^2 h} \right.$$

$$\left. \sum_{k=0}^K \|\|y_{k+1}^i - y_k^i - \sigma^2 \nabla \phi(y_k^i, kh)h\|^2 - \|y_{k+1}^i - y_k^i\|^2 \right] \quad (22)$$

Alternate between (18) and (22) several times. Above Var_n denotes the empirical variance across the n trajectories $\{y_k^i\}_{i=1}^n$ of the quantity inside $[\cdot]$. The loss (22), as the proof of Proposition 1 shows, comes from the fact that along the prior $X \sim \overrightarrow{\mathbb{P}}^{\nu, f}$, if ϕ is optimal,

$$\begin{aligned} & \log \left(\frac{d\overrightarrow{\mathbb{P}}^{\nu, f + \sigma^2 \nabla \phi_t}}{d\overrightarrow{\mathbb{P}}^{\nu, f}} \right) (X) = \quad (23) \\ & \int_0^T -\frac{\sigma^2}{2} \|\nabla \phi_t\|^2 dt + \int_0^T \sigma \nabla \phi_t^\top dW_t \stackrel{!}{=} \phi_T(X_T) - \phi_0(X_0) \end{aligned}$$

has to satisfy the factorization (45). And we discretized the Radon-Nikodym derivative (23) similar to how it was done in the KL divergence $D_{KL}(\overrightarrow{\mathbb{P}}^{\nu, \sigma^2 \nabla \phi} \|\overleftarrow{\mathbb{P}}^{\mu, -\sigma^2 \nabla \psi})$ (c.f. Lemma 1 for a similar derivation).

(3) Instead of the regularizer (22), another discretization of loss (b) using condition (23) can be a LSTD-like regularizer similar in spirit to (Liu et al., 2022):

$$\begin{aligned} & (19) + \lambda \cdot \frac{h}{n} \sum_{i=1}^n \sum_{k=0}^K \left| \phi(y_{k+1}^i, (k+1)h) - \phi(y_k^i, kh) + \right. \\ & \left. \frac{\sigma^2 h}{2} \|\nabla \phi(y_k^i, kh)\|^2 - \sigma \sqrt{h} \nabla \phi(y_k^i, kh)^\top Z_k^i \right|, \quad (24) \end{aligned}$$

where the Z_k^i 's are re-used from (21). The loss above can be justified with Lemma 4.

For the first three losses that we experiment (20), (22), (24), an analogous regularization on the backward drift involving $\nabla \psi$ is also possible (c.f. Remark 15).

(4) Separately-controlled loss (loss (c) from Proposition 1): Simulate (18) as before, with the n trajectories $\{x_k^i\}$, minimize over ϕ, ψ the following discretized loss (c.f. Lemma 1):

$$\begin{aligned} & \text{Var}_n [\psi(x_{K+1}^i, (K+1)h) + \phi(x_{K+1}^i, (K+1)h) - \log \mu(x_{K+1}^i)] + \\ & \text{Var}_n [\psi(x_0^i, 0) + \phi(x_0^i, 0) - \log \nu(x_0^i)] + \end{aligned} \quad (25)$$

$$\begin{aligned} & \frac{\lambda}{K+1} \text{Var}_n \left[\psi(x_{K+1}^i, (K+1)h) - \psi(x_0^i, 0) + \frac{1}{2\sigma^2 h} \right. \\ & \left. \sum_{k=0}^K \|x_{k+1}^i - x_k^i\|^2 - \|x_k^i - x_{k+1}^i - \sigma^2 h \nabla \psi(x_{k+1}^i, (k+1)h)\|^2 \right] \\ & + \frac{\lambda}{K+1} \text{Var}_n \left[\phi(x_0^i, 0) - \phi(x_{K+1}^i, (K+1)h) + \frac{1}{2\sigma^2 h} \right. \\ & \left. \sum_{k=0}^K \|x_{k+1}^i - x_k^i\|^2 - \|x_{k+1}^i - x_k^i - \sigma^2 h \nabla \phi(x_k^i, kh)\|^2 \right]. \end{aligned}$$

It consists of 4 variance terms, the last 2 coming from discretization of path measures (16). We alternate between simulating (18) and updating ϕ, ψ from (25). One can also consider SDE-based discretization for the last 2 terms but will incur additional Laplacian and divergence terms as suggested by Lemma 4, (66)-(67).

Comparison between discretized losses We emphasize that the discretized variance regularizers (22) and (74) wouldn’t be available without the path-wise stochastic process perspective. The FBSDE view (Lemma 4) will naturally lend to TD-like regularizers (24) and (75) similar to (Liu et al., 2022), but the crucial differences are: (1) we base the estimate on reference $\vec{\mathbb{P}}^{\nu, f}$ therefore there’s no need to differentiate through the generated trajectory when optimize the loss over $\nabla\phi$ or $\nabla\psi$; (2) (Liu et al., 2022) consider dynamics with mean-field interaction and different loss. The two discretized objectives (22)/(74) and (25) both enjoy variance reduction property as elaborated in Remark 3, without the need to evaluate expensive Laplacian terms (as the PDE-based PINN approach (20)/(73) or TD approach (75) would require).

4.2 Result

In our experiments, we picked the following 4 targets as benchmark as they capture different properties of distributions that can affect the training of the controls. These properties (multimodality, spatially varying curvature) pose challenges for MCMC methods and are ideal examples to demonstrate the differences between the regularizers.

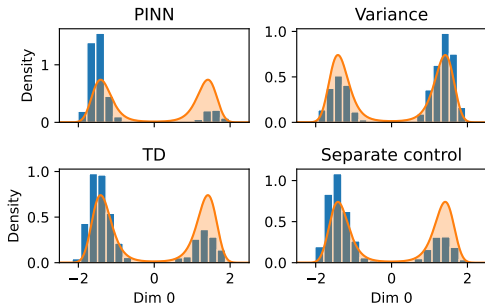


Figure 1: Weighted Marginal for Double Well

Table 1: $-\log Z$ Estimator (lower is better)

	PINN	Variance	TD	SC
Normal	6.318	2.883	2.014	1.305
Funnel	8.854	3.560	3.550	3.391
GMM	5.803	8.347	4.097	4.393
Double well	12.274	5.392	4.437	1.761

Additional supporting numerical experiments and details can be found in Appendix G. Across our experiments, we observe that our separately controlled loss (25) is generally much better compared to the PINN loss (20) that tends to exhibit mode-seeking behavior, while TD (24) and variance regularizer (22) can

sometimes be comparable. We also observe that the separately controlled loss is less sensitive to tuning parameters, and the training loss curve is often smoother.

From a practical standpoint, there are additional benefits for basing the methodology on a SB formulation. Since we have the knowledge that the optimal control vector field (1) takes the gradient form of a scalar function (i.e., divergence free therefore conservative); (2) satisfy the HJB equation which admit e.g., rotation equivariance: if $\phi(x, t), f(x, t)$ is a solution, $\phi(Rx, t), R^\top f(Rx, t)$ is another solution for a rotation matrix R . So in the example $f_t(x_t) = -x_t$, it simply implies that $\phi_t(x)$ is a radial function. These can be baked into the architecture as inductive bias for training in practical implementation (Kondor et al., 2018; Richter-Powell et al., 2022) so the NN can be sufficiently constrained to be more sample-efficient. This is an advantage compared to other diffusion-like samplers since this type of precise characterization of the optimal solution is something non-SB-bridge-based samplers do not admit.

5 CONCLUSION

We exploited the connections between diffusion generative modeling, stochastic control and optimal transport, with the goal of sampling from high-dimensional, complex distributions in mind. This is orthogonal to MCMC-based approaches, and is accomplished by a more “learning-driven” methodology on the optimal control / drift that can be trained with a suitable control objective. While there are a lot of flexibility in the design (that also makes the case for SB more compelling than existing pathwise samplers mentioned in Section 2.2), we have illustrated that careful choice is needed for both numerical implementation and generalizability of the framework.

More broadly, the mapping between target $p_{\text{target}}(x)$ and control $\phi(x, t)$ can be thought of as a form of operator learning mapping between functions in infinite dimensional space, for which universal approximation theorems have emerged recently for various neural network architectures (De Ryck and Mishra, 2022). More specifically, one can view the task as learning the solution operator of the coupled PDEs (33)-(34). This also points to the fact that our SB-based methodology can effectively leverage available data (i.e., supervised $\mu, \nabla\phi$ pairs) to generalize across tasks rather than being a task-specific problem only, such as the other diffusion-type samplers that train for path-measure consistency. Application-wise, exploiting such methods in the context of molecular dynamics simulation for sampling transition path is also exciting and development is already underway (Holdijk et al., 2023).

References

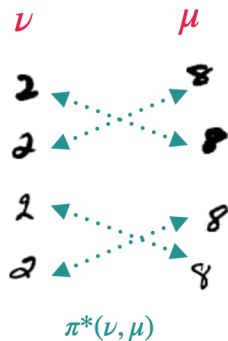
- Jean-David Benamou and Yann Brenier. A computational fluid mechanics solution to the Monge-Kantorovich mass transfer problem. *Numerische Mathematik*, 84(3):375–393, 2000.
- Julius Berner, Lorenz Richter, and Karen Ullrich. An optimal control perspective on diffusion-based generative modeling. *arXiv preprint arXiv:2211.01364*, 2022.
- Kenneth F Caluya and Abhishek Halder. Wasserstein proximal algorithms for the Schrödinger bridge problem: Density control with nonlinear drift. *IEEE Transactions on Automatic Control*, 67(3):1163–1178, 2021.
- Ricky TQ Chen, Yulia Rubanova, Jesse Bettencourt, and David K Duvenaud. Neural ordinary differential equations. *Advances in neural information processing systems*, 31, 2018.
- Tianrong Chen, Guan-Horng Liu, and Evangelos Theodorou. Likelihood Training of Schrödinger Bridge using Forward-Backward SDEs Theory. In *International Conference on Learning Representations*, 2021a.
- Tianrong Chen, Guan-Horng Liu, Molei Tao, and Evangelos Theodorou. Deep momentum multi-marginal Schrödinger bridge. *Advances in Neural Information Processing Systems*, 36, 2023.
- Yongxin Chen, Tryphon T Georgiou, and Michele Pavon. Stochastic control liaisons: Richard Sinkhorn meets Gaspard Monge on a Schrödinger Bridge. *SIAM Review*, 63(2):249–313, 2021b.
- Valentin De Bortoli, James Thornton, Jeremy Heng, and Arnaud Doucet. Diffusion Schrödinger bridge with applications to score-based generative modeling. *Advances in Neural Information Processing Systems*, 34:17695–17709, 2021.
- Tim De Ryck and Siddhartha Mishra. Generic bounds on the approximation error for physics-informed (and) operator learning. *Advances in Neural Information Processing Systems*, 35:10945–10958, 2022.
- Tim Dockhorn, Arash Vahdat, and Karsten Kreis. Score-Based Generative Modeling with Critically-Damped Langevin Diffusion. In *International Conference on Learning Representations (ICLR)*, 2022.
- Arnaud Doucet, Will Grathwohl, Alexander G Matthews, and Heiko Strathmann. Score-based diffusion meets annealed importance sampling. *Advances in Neural Information Processing Systems*, 35:21482–21494, 2022.
- Lars Holdijk, Yuanqi Du, Ferry Hooft, Priyank Jaini, Berend Ensing, and Max Welling. Stochastic Optimal Control for Collective Variable Free Sampling of Molecular Transition Paths. *Advances in Neural Information Processing Systems*, 36, 2023.
- Aapo Hyvärinen and Peter Dayan. Estimation of non-normalized statistical models by score matching. *Journal of Machine Learning Research*, 6(4), 2005.
- Hicham Janati, Boris Muzellec, Gabriel Peyré, and Marco Cuturi. Entropic optimal transport between unbalanced Gaussian measures has a closed form. *Advances in neural information processing systems*, 33:10468–10479, 2020.
- Risi Kondor, Zhen Lin, and Shubhendu Trivedi. Clebsch–gordan nets: a fully fourier space spherical convolutional neural network. *Advances in Neural Information Processing Systems*, 31, 2018.
- Christian Léonard. A survey of the Schrödinger problem and some of its connections with optimal transport. *Discrete and Continuous Dynamical Systems-Series A*, 34(4):1533–1574, 2014.
- Guan-Horng Liu, Tianrong Chen, Oswin So, and Evangelos Theodorou. Deep generalized Schrödinger bridge. *Advances in Neural Information Processing Systems*, 35:9374–9388, 2022.
- Nikolas Nüsken and Lorenz Richter. Interpolating between BSDEs and PINNs: deep learning for elliptic and parabolic boundary value problems. *arXiv preprint arXiv:2112.03749*, 2021.
- Michele Pavon, Giulio Trigila, and Esteban G Tabak. The Data-Driven Schrödinger Bridge. *Communications on Pure and Applied Mathematics*, 74(7):1545–1573, 2021.
- Stefano Peluchetti. Diffusion Bridge Mixture Transports, Schrödinger Bridge Problems and Generative Modeling. *arXiv preprint arXiv:2304.00917*, 2023.
- Gabriel Peyré and Marco Cuturi. Computational optimal transport: With applications to data science. *Foundations and Trends in Machine Learning*, 11(5-6):355–607, 2019.
- Maziar Raissi, Paris Perdikaris, and George E Karniadakis. Physics-informed neural networks: A deep learning framework for solving forward and inverse problems involving nonlinear partial differential equations. *Journal of Computational physics*, 378:686–707, 2019.
- Lorenz Richter, Julius Berner, and Guan-Horng Liu. Improved sampling via learned diffusions. *arXiv preprint arXiv:2307.01198*, 2023.
- Jack Richter-Powell, Yaron Lipman, and Ricky TQ Chen. Neural conservation laws: A divergence-free perspective. *Advances in Neural Information Processing Systems*, 35:38075–38088, 2022.

- Erwin Schrödinger. *Über die umkehrung der naturgesetze*. Sitzungsberichte der preussischen Akademie der Wissenschaften, physikalische mathematische Klasse, 1931.
- Yuyang Shi, Valentin De Bortoli, Andrew Campbell, and Arnaud Doucet. Diffusion Schrödinger bridge matching. *Advances in Neural Information Processing Systems*, 36, 2023.
- Yang Song, Jascha Sohl-Dickstein, Diederik P Kingma, Abhishek Kumar, Stefano Ermon, and Ben Poole. Score-Based Generative Modeling through Stochastic Differential Equations. In *International Conference on Learning Representations*, 2020.
- Sep Thijssen and HJ Kappen. Path integral control and state-dependent feedback. *Physical Review E*, 91(3):032104, 2015.
- Belinda Tzen and Maxim Raginsky. Theoretical guarantees for sampling and inference in generative models with latent diffusions. In *Conference on Learning Theory*, pages 3084–3114. PMLR, 2019.
- Francisco Vargas and Nikolas Nüsken. Transport, Variational Inference and Diffusions: with Applications to Annealed Flows and Schrödinger Bridges. *arXiv preprint arXiv:2307.01050*, 2023.
- Francisco Vargas, Pierre Thodoroff, Austen Lamacraft, and Neil Lawrence. Solving Schrödinger bridges via maximum likelihood. *Entropy*, 23(9): 1134, 2021.
- Francisco Vargas, Will Sussman Grathwohl, and Arnaud Doucet. Denoising Diffusion Samplers. In *The Eleventh International Conference on Learning Representations*, 2022.
- Qinsheng Zhang and Yongxin Chen. Path Integral Sampler: A Stochastic Control Approach For Sampling. In *International Conference on Learning Representations*, 2021.
- Mo Zhou, Jiequn Han, and Jianfeng Lu. Actor-critic method for high dimensional static Hamilton–Jacobi–Bellman partial differential equations based on neural networks. *SIAM Journal on Scientific Computing*, 43(6):A4043–A4066, 2021.

Control, Transport and Sampling Towards Better Loss Design: Supplementary Materials

A ADDITIONAL MOTIVATION & PRACTICAL CONSIDERATION

The main application we have in mind is for gradient-free sampling but the very same methodology can be applied for optimal transport and stochastic control applications. To give a concrete example, one might have handwriting of 2 digits collected from a group of individuals as the 2 marginals, the coupling $\pi^*(\nu, \mu)$ identified by the SB will put most of its mass on the digits written by the same people, therefore this kind of matching capability has applications beyond marginal sampling at the terminal time. The optimal control aspect of the SB trajectory finds application in e.g., transition path / rare-event sampling (Holdijk et al., 2023), which is a well-known challenge in computational chemistry.



will put most of the mass on **dashed** pairs

Figure 2: Optimal Transport Between Fixed Marginals

Beyond being able to leverage special NN architecture, from a differential programming perspective, the “precise understanding of the solution” for SB is also beneficial. At optimality after our training procedure, since we know the optimal control solves a convex optimization problem ((35)-(36) is not convex in ρ, u as written, but it can be turned into a convex problem in a new set of parameters $\rho, m = \rho u$), if we perturb the target density $\mu(\cdot)$ slightly, one can leverage implicit differentiation to work out a perturbation on the optimal control $u_t(\cdot)$ locally, without differentiating through the solver that is used for training. This is because one can view the operation as a mapping $\mu \mapsto (\rho_t, u_t)$ through the KKT condition. This notion of uniqueness and optimality imply our SB formulation can avoid expensive retraining when deployed in multiple similar instances, in contrast to other diffusion-style samplers (Vargas et al., 2022; Richter et al., 2023). We view having an optimality baked into the solution as ideal for blending problem structure into generic off-the-shelf machine learning methods.

B VARIOUS PERSPECTIVES ON THE SCHRÖDINGER BRIDGE PROBLEM

Most of these can be traced out in (Léonard, 2014; Chen et al., 2021b), which has its roots in statistical mechanics (Schrödinger, 1931) (and in modern terms, closely related to large-deviation results via Sanov’s theorem). For us however, the following perspectives will be more fruitful.

(1) Mixture of pinned diffusions (weights given by π^*) can be seen by disintegration of path measure:

$$D_{KL}(P\|Q) = D_{KL}(P_{0T}\|Q_{0T}) + \int D_{KL}(P^{zx}\|Q^{zx}) dP_{0T}(z, x). \quad (26)$$

Since the only constraints are on the two end-points (13) is therefore equivalent to (27), by choosing $P^{zx} = Q^{zx}$. The optimal solution takes the form $P^* = \pi^* Q^{zx}$, which means one can sample from $(z, x) \sim \pi^* \in \Pi_{\nu, \mu}$, and sample from the bridges conditioned on the end-points at $t = 0, T$.

(2) It has the interpretation of entropy-regularized optimal transport (Peyré and Cuturi, 2019) when $f = 0$: in terms of static formulation because of (26), if the reference Q is simply the Wiener process (accordingly $r(x|z) \propto e^{-\frac{1}{2T}\|x-z\|^2}$),

$$\begin{aligned} \pi^*(z, x) &= \arg \min_{\pi_z=\nu, \pi_x=\mu} D_{KL}(\pi(z, x)\|r(z, x)) \\ &= \arg \min_{\pi_z=\nu, \pi_x=\mu} \mathbb{E}_{z \sim \nu} [D_{KL}(\pi(x|z)\|r(x|z))] + D_{KL}(\nu(z)\|r(z)) \\ &= \arg \min_{\pi_z=\nu, \pi_x=\mu} \int \frac{1}{2} \|x - z\|^2 \pi(z, x) dx dz + T \int \pi(z, x) \log \pi(z, x) dx dz \\ &= \arg \min_{\pi_z=\nu, \pi_x=\mu} \underbrace{\int \frac{1}{2} \|x - z\|^2 \pi(z, x) dx dz}_{\mathcal{C}(z, x)} + T \underbrace{\int \pi(z, x) \log \frac{\pi(z, x)}{\nu(z) \otimes \mu(x)} dx dz}_{D_{KL}(\pi(z, x)\|\nu(z) \otimes \mu(x))}, \end{aligned} \quad (27)$$

where the first term is nothing but the definition of the Wasserstein-2 distance (and optimal transport with quadratic cost in the sense of Kantorovich). The second entropy term favors independent coupling $\nu \otimes \mu$. This is a Lagrangian description of the transport. Different choices of $r(x|z)$ transition will induce different transport costs. The objective above can also be written as

$$\arg \min_{\pi_z=\nu, \pi_x=\mu} D_{KL} \left(\pi(z, x) \parallel e^{-\mathcal{C}(z, x)/2T} \nu(z) \otimes \mu(x) \right).$$

In terms of dynamical formulation, via Girsanov’s theorem on path measure, with the controlled dynamics as

$$dX_t = [f_t(X_t) + \sigma u_t(X_t)] dt + \sigma dW_t,$$

(13) can be reformulated as a *constrained* problem:

$$P^* = \arg \min_P \mathbb{E}_{X \sim \vec{\mathbb{P}}^{\nu, f + \sigma u}} \left[\frac{1}{2} \int_0^T \|u_t(X_t)\|^2 dt \mid \vec{\mathbb{P}}_T^{\nu, f + \sigma u} = \mu \right]. \quad (28)$$

Or a *regularized* Benamou-Brenier fluid-dynamics (Benamou and Brenier, 2000) analogy of the optimal transport

$$\inf_{\rho, v} \int_{\mathbb{R}^d} \int_0^T \left[\frac{1}{2} \|v_t(X_t) - \bar{v}_t(X_t)\|^2 + \frac{\sigma^4}{8} \left\| \nabla \log \frac{\rho_t(X_t)}{\bar{\rho}_t(X_t)} \right\|^2 \right] \rho_t(X_t) dt dx \quad (29)$$

$$\text{s.t. } \frac{\partial \rho_t}{\partial t} + \nabla \cdot (\rho_t v_t) = 0, \rho_0 = \nu, \rho_T = \mu. \quad (30)$$

Above $\bar{v}_t = f_t - \frac{\sigma^2}{2} \nabla \log \bar{\rho}_t$ is the velocity field of the prior process, and we see the penalization results in an additional relative Fisher information term. Since v^* is a velocity field in the continuity equation, it means a deterministic evolution (i.e., ODE) as

$$\dot{X}_t = v_t(X_t), X_0 \sim \nu$$

will have $X_t \sim \rho_t$, the optimal entropic interpolation flow, which gives an Eulerian viewpoint.

(3) Optimal control views the problem as steering ν at $t = 0$ to μ at $t = T$ with minimal control effort. The value function (i.e., optimal cost-to-go)

$$V(x, t) := \min_u \mathbb{E}_u \left[\frac{1}{2} \int_t^T \|u_s(X_s)\|^2 ds \mid X_t^u = x, X_T^u \sim \mu \right] \quad (31)$$

with the expectation taken over the stochastic dynamics

$$dX_t^u = [f_t(X_t^u) + \sigma u_t(X_t^u)]dt + \sigma dW_t, \quad X_0^u \sim \nu \quad (32)$$

should satisfy the Hamilton-Jacobi-Bellman equation via the dynamical programming principle

$$\frac{\partial V(x, t)}{\partial t} + f_t(x)^\top \nabla V(x, t) + \frac{\sigma^2}{2} \Delta V(x, t) - \frac{\sigma^2}{2} \|\nabla V(x, t)\|^2 = 0, \quad (33)$$

where the optimal control $u_t^*(X_t) = -\sigma \nabla V(X_t, t)$ and gives the unique solution $(\rho_t^u)_{t \geq 0}$ solving

$$\frac{\partial \rho_t^u}{\partial t} = -\nabla \cdot (\rho_t^u (f_t - \sigma^2 \nabla V_t)) + \frac{\sigma^2}{2} \Delta \rho_t^u, \quad \rho_0^u \sim \nu, \rho_T^u \sim \mu. \quad (34)$$

The two *coupled* PDEs, Fokker-Planck (34) and HJB (33) are also the KKT optimality condition of

$$\inf_{\rho, u} \int_{\mathbb{R}^d} \int_0^T \frac{1}{2} \|u_t(X_t)\|^2 \rho_t(X_t) dt dx \quad (35)$$

$$\text{s.t. } \frac{\partial \rho_t}{\partial t} + \nabla \cdot (\rho_t (f_t + \sigma u_t)) = \frac{\sigma^2}{2} \Delta \rho_t, \quad \rho_0 = \nu, \rho_T = \mu \quad (36)$$

where again the optimal $u^* = -\sigma \nabla V$ is of gradient type. Above the Laplacian is responsible for the diffusion part, and (35)-(36) is related to (29)-(30) via a change of variable. One might try to design schemes by forming the Lagrangian for the above (35)-(36), and solve the resulting saddle-point problem, but this deviates somewhat from our pathwise narrative.

Remark 6 (Langevin). Compared to the Langevin SDE $dX_t = -\nabla f(X_t)dt + \sqrt{2}dW_t$, which only involves forward-evolving density characterization and reaches equilibrium as $T \rightarrow \infty$, the controlled SDE (32) is time-inhomogeneous and involves two PDEs (33)-(34). Langevin also has a backward Kolmogorov evolution for the expectation of a function g : let $V(x, t) = \mathbb{E}[g(X_T) \mid X_t = x]$, we have $\partial_t V(x, t) - \nabla f(x)^\top \nabla V(x, t) + \Delta V(x, t) = 0$ with $V(x, T) = g(x)$, but it is *de-coupled* from the Fokker-Planck equation $\partial_t \rho_t - \nabla \cdot (\rho_t \nabla f) - \Delta \rho_t = 0$ with $\rho_0 = \nu$.

Remark 7 (Bound on optimal objective). Notice that in fact

$$\min_u \mathbb{E}_u \left[\int_0^T \frac{1}{2} \|u_t(X_t)\|^2 dt - \log \frac{p_{\text{target}}}{Q_T}(X_T) \right] \geq 0, \quad (37)$$

which means we know a lower bound on the minimum of our losses (a) and (d) in Proposition 1. This holds since for the controlled process P ,

$$D_{KL}(P \parallel Q) = \mathbb{E}_u \left[\int_0^T \frac{1}{2} \|u_t(X_t)\|^2 dt \right] = \mathbb{E}_u \left[\frac{1}{2} \int_0^T \|u_t(X_t)\|^2 dt - \log \frac{p_{\text{target}}}{Q_T}(X_T) \right] + D_{KL}(p_{\text{target}} \parallel Q_T),$$

which gives the claim by the data processing inequality $D_{KL}(p_{\text{target}} \parallel Q_T) \leq D_{KL}(P \parallel Q)$. A special instance is when ν is δ_0 a fixed Dirac delta and the reference process is simply Brownian motion $f_t = 0$. In this case, the optimal drift u^* is known to be the Föllmer drift (Tzen and Raginsky, 2019; Zhang and Chen, 2021) and can be computed explicitly as (picking $T = 1$ for simplicity below)

$$u_t^*(x) = \arg \min_u \mathbb{E}_{X \sim \vec{\mathbb{P}}^{\nu, \sigma u}} \left[\int_0^1 \frac{1}{2} \|u_s(X_s)\|^2 ds + \log \left(\frac{Q_1}{p_{\text{target}}} \right) (X_1) \right] \quad (38)$$

$$\begin{aligned}
 &= \nabla \log \mathbb{E}_X \left[\frac{d\mu}{dQ_1}(X_1) \mid X_t = x \right] \\
 &= \nabla \log \mathbb{E}_{z \sim \mathcal{N}(0, \sigma^2 I)} \left[\frac{d\mu}{d\mathcal{N}(0, \sigma^2 I)}(x + \sqrt{1-t}z) \right],
 \end{aligned} \tag{39}$$

where the expectation in (39) is taken w.r.t the reference measure – Wiener process in this case; and it follows from Doob’s h -transform that the reverse drift $v_t^*(x) = x/t$ is also analytical. This is technically speaking a half-bridge where one can show $P_t^*(X_t) = Q(X_t | X_T) p_{\text{target}}(X_T)$ and equality in (37) holds exactly. (38) gives an intuitive explanation of the optimally-controlled process, with the first part corresponding to the running cost and the second part to the terminal cost.

(4) The non-negative functions ϕ, ψ (which are closely related to the dual potentials f, g from (44) below) yield optimal forward/backward drifts: It holds that the optimal curve admits the representation

$$\log \rho_t = \log \phi_t + \log \psi_t \quad \text{for all } t \tag{40}$$

and solving the boundary-coupled linear PDE system on the control

$$\frac{\partial \phi_t}{\partial t} = -\frac{\sigma^2}{2} \Delta \phi_t - \nabla \phi_t^\top f_t, \quad \frac{\partial \psi_t}{\partial t} = \frac{\sigma^2}{2} \Delta \psi_t - \nabla \cdot (\psi_t f_t) \quad \text{for } \phi_0 \psi_0 = p_{\text{prior}}, \phi_T \psi_T = p_{\text{target}} \tag{41}$$

gives two SDEs for the optimal curve in (13):

$$dX_t = [f_t(X_t) + \sigma^2 \nabla \log \phi_t(X_t)] dt + \sigma d\overrightarrow{W}_t, \quad X_0 \sim \nu \tag{42}$$

$$dX_t = [f_t(X_t) - \sigma^2 \nabla \log \psi_t(X_t)] dt + \sigma d\overleftarrow{W}_t, \quad X_T \sim \mu. \tag{43}$$

Note that equations (42)-(43) are time reversals of each other and obey Nelson’s identity thanks to (40). The transformation (40)-(41) that involves $(\rho_t^*, u_t^*) = (\rho_t^*, -\sigma \nabla V_t) \mapsto (\phi_t, \psi_t)$ is a typical $\log \leftrightarrow \exp$ Hopf-Cole change-of-variable from (33)-(34). These PDE optimality results can be found in (Caluya and Halder, 2021).

Remark 8 (Boundary condition). In rare cases, such as those from Föllmer drift (39), the PDE system (41) (or (33)-(34)) may decouple and the drift can be expressed analytically. But the boundary conditions of (33)-(34) is atypical for control problems, which generally would have (34) specified at initial time and runs forward, with (33) specified at the terminal and runs backward. The PDE dynamics (41) also takes similar form as those from Remark 6 but with slightly unusually coupled boundary conditions.

(5) Factorization of the optimal coupling: in fact it is always the case that

$$\frac{d\pi^*}{dr}(X_0, X_T) = e^{f(X_0)} e^{g(X_T)} \quad r\text{-a.s.} \tag{44}$$

Moreover under mild conditions if there exists π, f, g for which such decomposition holds and $\pi_0 = \nu, \pi_T = \mu$, π must be optimal – such condition (44) is *necessary and sufficient* for characterizing the solution to the SB problem. (44) together with (26) give that (which can also be thought of as re-weighting on the path space)

$$\frac{dP^*}{dQ}(X_{0:T}) = e^{f(X_0)} e^{g(X_T)} \quad Q\text{-a.s.}, \tag{45}$$

where the f and g obey the Schrödinger system

$$e^{f(x_0)} \int r(X_0 = x_0, X_T) e^{g(X_T)} dX_T = p_{\text{prior}}(x_0), \quad e^{g(x_T)} \int e^{f(X_0)} r(X_0, X_T = x_T) dX_0 = p_{\text{target}}(x_T). \tag{46}$$

The ϕ, ψ in (42)-(43) can also be expressed as a conditional expectation:

$$\begin{aligned}
 \phi_t(x) &\stackrel{(\#)}{=} \int e^{g(X_T)} r(X_T | X_t = x) dX_T \stackrel{(*)}{=} \int_{\mathbb{R}^d} \phi_T(X_T) r(X_T | X_t = x) dX_T, \\
 \psi_t(x) &\stackrel{(\#)}{=} \int e^{f(X_0)} r(X_t = x, X_0) dX_0 \stackrel{(*)}{=} \int_{\mathbb{R}^d} \psi_0(X_0) r(X_t = x | X_0) dX_0
 \end{aligned}$$

for $t \in [0, T]$, where (#) can be verified with (46), (40). And for the second transition (*), one can simply check using the relationship (#) that

$$\psi_0(X_0) = e^{f(X_0)} r(X_0), \phi_T(X_T) = e^{g(X_T)}$$

therefore

$$\frac{dP^*}{dQ}(X_{0:T}) = e^{f(X_0)} e^{g(X_T)} = \frac{\psi_0(X_0)\phi_T(X_T)}{r(X_0)} = \frac{\psi_0(X_0)\phi_T(X_T)}{p_{\text{prior}}(X_0)} \quad (47)$$

is how the optimal coupling should factorize. This representation of ϕ_t, ψ_t as the conditional expectation (*) can be seen with the Feynman-Kac formula on (41) as well. But in general, the transition kernel of the un-controlled process $r(\cdot)$, or more importantly the terminals ϕ_T, ψ_0 are not available analytically for solving for ϕ_t, ψ_t as (*).

Remark 9. Such factorization property (44) is maintained by Sinkhorn algorithm (that updates f, g as iteration proceeds), which is well-known to converge to the optimal coupling eventually.

(6) Equation (42) means the optimal v_t^* in the continuity equation (30) is $f_t + \sigma^2 \nabla \log \phi_t - \frac{\sigma^2}{2} \nabla \log \rho_t = f_t + \frac{\sigma^2}{2} \nabla \log \frac{\phi_t}{\psi_t}$, which gives the probability flow ODE for this dynamics:

$$dX_t = f_t(X_t) + \frac{\sigma^2}{2} (\nabla \log \phi_t(X_t) - \nabla \log \psi_t(X_t)) dt, \quad X_0 \sim \nu, \quad (48)$$

in the sense that the time marginals $\rho_t^{(48)} = \rho_t^{(42)} = \rho_t^{(43)} = P_t^{(13)}$ all agree. Moreover, using the instantaneous change of variables formula (Chen et al., 2018), we also have

$$\log \rho_T(X_T) = \log \rho_0(X_0) - \int_0^T \nabla \cdot f_t(X_t) dt - \frac{\sigma^2}{2} \int_0^T \nabla \cdot (\nabla \log \phi_t(X_t) - \nabla \log \psi_t(X_t)) dt, \quad (49)$$

which will be useful in Proposition 2 for estimating the normalizing constant. Note that in (49) both the density and the point at which we are evaluating is changing.

Remark 10 (Minimum control energy). The stochastic control formulation makes it clear that the trajectory we are trying to recover is a meaningful one in the sense of minimal effort. If one were to switch the order of P and Q in (13), the optimal control problem becomes (e.g., for $f = 0$)

$$\inf_u \mathbb{E} \left[\int_0^T \frac{1}{2} \|u_t(X_t)\|^2 dt \right]$$

s.t. $dX_t = \sigma u_t(X_t) dt + \sigma dW_t, X_0 \sim \nu, X_T \sim \mu$

for the expectation taken over the reference process, instead of the controlled state density ρ_t^u , which is not very intuitive. The slightly non-conventional aspect of this control problem is the fixed terminal constraint.

To briefly summarize, all these different viewpoints explore the deep connections between PDEs (controls) and SDEs (diffusions) in one way or another.

C ADDITIONAL RELATED WORK: NATURAL ATTEMPTS FOR SOLVING SB

In this section we discuss several natural attempts with the intention of adapting the SB formalism for sampling from un-normalized densities.

- Iterative proportional fitting (IPF) / Sinkhorn performs iterative projection as

$$P^{(1)} = \arg \min_{Q \in \mathcal{P}(\nu, \cdot)} D_{KL}(Q \| P^{(0)}) = \frac{P^{(0)} \nu}{P_0^{(0)}}, \quad P^{(0)} = \arg \min_{Q \in \mathcal{P}(\cdot, \mu)} D_{KL}(Q \| P^{(1)}) = \frac{P^{(1)} \mu}{P_T^{(1)}} \quad (50)$$

i.e., one solves half-bridges using drifts learned from the last trajectory transition rollout, and only the end point differ. But since we don't have samples from μ , neither the score function nor the succeeding IPF

updates/refinements can be implemented. In fact, the first iteration of the IPF proposal in (De Bortoli et al., 2021; Vargas et al., 2021) precisely corresponds to the score-based diffusion proposal in (Song et al., 2020). However, there is a connection between IPF and a path space EM implementation formulated in terms of drifts that rely on change in the KL direction: recall under mild assumptions

$$\arg \min_{\phi} D_{KL}(\overrightarrow{\mathbb{P}}^{\nu, f + \sigma^2 \nabla \phi} \parallel \overleftarrow{\mathbb{P}}^{\mu, f + \sigma^2 \nabla \psi}) = \arg \min_{\phi} D_{KL}(\overleftarrow{\mathbb{P}}^{\mu, f + \sigma^2 \nabla \psi} \parallel \overrightarrow{\mathbb{P}}^{\nu, f + \sigma^2 \nabla \phi}).$$

Using this fact, it is shown in (Vargas and Nüsken, 2023) that coordinate descent on the objective $\min_{\phi, \psi} D_{KL}(\overrightarrow{\mathbb{P}}^{\nu, f + \sigma^2 \nabla \phi} \parallel \overleftarrow{\mathbb{P}}^{\mu, f + \sigma^2 \nabla \psi})$, when initializing at $\phi = 0$ (i.e., the prior), is a valid strategy for solving (13), as it gives the same sequence of path measures as (50).

Lemma 2 (Optimization of drifts of EM (Vargas and Nüsken, 2023)). *The alternating scheme initialized with $\phi_0 = 0$ converge to P^* (i.e., the coupling at time $t = 0, T$ is optimal):*

$$\psi_n = \arg \min_{\psi} D_{KL}(\overrightarrow{\mathbb{P}}^{\nu, f + \sigma^2 \nabla \phi_{n-1}} \parallel \overleftarrow{\mathbb{P}}^{\mu, f + \sigma^2 \nabla \psi}) \quad (51)$$

$$\phi_n = \arg \min_{\phi} D_{KL}(\overrightarrow{\mathbb{P}}^{\nu, f + \sigma^2 \nabla \phi} \parallel \overleftarrow{\mathbb{P}}^{\mu, f + \sigma^2 \nabla \psi_n}). \quad (52)$$

Moreover, both updates are implementable assuming samples from ν is available, which resolves non-uniqueness of the two parameter loss $\min_{\phi, \psi} D_{KL}(\overrightarrow{\mathbb{P}}^{\nu, f + \sigma^2 \nabla \phi} \parallel \overleftarrow{\mathbb{P}}^{\mu, f + \sigma^2 \nabla \psi})$ in an algorithmic manner (fixing one direction of the drift at a time).

Remark 11 (Benefit of joint training). Lemma 2 above also shows that the prior only enters in the first step, therefore as it proceeds, the prior influence tends to be ignored as error accumulates – this aspect is different from our loss proposals in Proposition 1. Another advantage of our joint minimization procedure compared to an iterative sequential IPF method is that while the equivalence of EM and IPF will no longer hold for neural network models not expressive enough (therefore the convergence does not immediately carry over), one could still estimate the normalizing constant / sample from the target with a sub-optimal control learned from the losses proposed in Proposition 1 with e.g., important weights (c.f. (93)).

- Some alternatives to solve SB do not require analytical expression for μ : diffusion mixture matching (Peluchetti, 2023; Shi et al., 2023) tilts the product measure $\nu \otimes \mu$ towards optimality gradually by learning a slightly different term than the score, and alternate between such Markovian and reciprocal projection. Data-driven bridge (Pavon et al., 2021) aims at setting up a fixed point recursion on the SB system (46) for finding the optimal ϕ^*, ψ^* , but both rely on (1) the availability of samples from μ (as well as ν) to estimate various quantities for implementation; (2) tractable bridge distribution/Markov kernel for the reference $Q(\cdot | X_0, X_T)$. In fact a different initialization from the reference Q using method in (Shi et al., 2023) will reduce to IPF.
- The work of (Caluya and Halder, 2021) investigated the case where the reference process has a gradient drift (i.e., $f = -\nabla U$) and reduce the optimal control task to solving a high-dimensional PDE subject to initial-value constraint (c.f. Eqn (33) and (47) therein). However, solving PDEs is largely regarded to be computationally more demanding than simulating SDEs.

D MISSING PROOFS AND CALCULATIONS

We give the likelihood ratio calculation Lemma 3 below, which is closely related to those from (Richter et al., 2023; Vargas and Nüsken, 2023) and repeatedly used in our losses.

Lemma 3 (Forward / Backward path-space likelihood ratio). *Written solely in terms of the drifts, the KL divergence $D_{KL}(\overrightarrow{\mathbb{P}}^{\nu, f+\sigma u} \parallel \overleftarrow{\mathbb{P}}^{\mu, f+\sigma v})$ becomes*

$$\mathcal{L}_{KL}(u, v) = \mathbb{E}_{X \sim \overrightarrow{\mathbb{P}}^{\nu, f+\sigma u}} \left[\int_0^T \frac{1}{2} \|u_t(X_t) - v_t(X_t)\|^2 - \nabla \cdot (f_t + \sigma v_t)(X_t) dt + \log \frac{d\nu(X_0)}{d\mu(X_T)} \right] + \log Z. \quad (53)$$

And the log-variance divergence over the same two path measures can be evaluated to be

$$\text{Var}_{X \sim \overrightarrow{\mathbb{P}}^{\nu, f+\sigma u}} \left[\int_0^T \frac{1}{2} \|u_t(X_t) - v_t(X_t)\|^2 - \nabla \cdot (f_t + \sigma v_t)(X_t) dt + \log \frac{d\nu(X_0)}{d\mu(X_T)} + \int_0^T (u_t - v_t)(X_t) \overrightarrow{dW}_t \right].$$

The reverse one $D_{KL}(\overleftarrow{\mathbb{P}}^{\mu, f+\sigma v} \parallel \overrightarrow{\mathbb{P}}^{\nu, f+\sigma u})$ becomes up to constant

$$\mathbb{E}_{X \sim \overleftarrow{\mathbb{P}}^{\mu, f+\sigma v}} \left[\int_0^T \frac{1}{2} \|v_t(X_t) - u_t(X_t)\|^2 + \nabla \cdot (f_t + \sigma u_t)(X_t) dt + \log \frac{d\mu(X_T)}{d\nu(X_0)} \right].$$

Proof of Lemma 3. We give a few equivalent expressions for the Radon-Nikodym derivative.

Argument due to (Vargas and Nüsken, 2023): Starting with Proposition 2.2 of (Vargas and Nüsken, 2023), in the general case of reference

$$dX_t = \sigma r_t^+(X_t) dt + \sigma \overrightarrow{dW}_t, \quad X_0 \sim \Gamma_0 \quad dX_t = \sigma r_t^-(X_t) dt + \sigma \overleftarrow{dW}_t, \quad X_T \sim \Gamma_T \quad (54)$$

where $\overrightarrow{\mathbb{P}}^{\Gamma_0, \sigma r^+} = \overleftarrow{\mathbb{P}}^{\Gamma_T, \sigma r^-}$, it is shown $\overrightarrow{\mathbb{P}}^{\nu, f+\sigma u}$ almost surely,

$$\begin{aligned} \log \left(\frac{d\overrightarrow{\mathbb{P}}^{\nu, f+\sigma u}}{d\overleftarrow{\mathbb{P}}^{\mu, f+\sigma v}} \right) (X) &= \log \left(\frac{d\nu}{d\Gamma_0} \right) (X_0) - \log \left(\frac{d\mu}{d\Gamma_T} \right) (X_T) + \log Z \\ &+ \frac{1}{\sigma^2} \int_0^T (f_t + \sigma u_t - \sigma r_t^+)(X_t) \left(\overrightarrow{dX}_t - \frac{1}{2} (f_t + \sigma u_t + \sigma r_t^+)(X_t) dt \right) \end{aligned} \quad (55)$$

$$- \frac{1}{\sigma^2} \int_0^T (f_t + \sigma v_t - \sigma r_t^-)(X_t) \left(\overleftarrow{dX}_t - \frac{1}{2} (f_t + \sigma v_t + \sigma r_t^-)(X_t) dt \right). \quad (56)$$

One can use (8) to convert the backward integral to a forward one with an additional divergence term

$$\begin{aligned} D_{KL}(\overrightarrow{\mathbb{P}}^{\nu, f+\sigma u} \parallel \overleftarrow{\mathbb{P}}^{\mu, f+\sigma v}) &= \mathbb{E}_{X \sim \overrightarrow{\mathbb{P}}^{\nu, f+\sigma u}} \left[\log \left(\frac{d\overrightarrow{\mathbb{P}}^{\nu, f+\sigma u}}{d\overleftarrow{\mathbb{P}}^{\mu, f+\sigma v}} \right) (X) \right] \\ &= \mathbb{E}_{X \sim \overrightarrow{\mathbb{P}}^{\nu, f+\sigma u}} \left[\log \left(\frac{d\nu}{d\Gamma_0} \right) (X_0) - \log \left(\frac{d\mu}{d\Gamma_T} \right) (X_T) + \log Z \right. \\ &+ \frac{1}{2\sigma^2} \int_0^T (f_t + \sigma u_t - \sigma r_t^+)(X_t)^\top (f_t + \sigma u_t - \sigma r_t^+)(X_t) dt \\ &- \frac{1}{\sigma^2} \int_0^T (f_t + \sigma v_t - \sigma r_t^-)(X_t)^\top \left(\frac{1}{2} f_t + \sigma u_t - \frac{\sigma}{2} v_t - \frac{\sigma}{2} r_t^- \right) (X_t) dt - \int_0^T \nabla \cdot (f_t + \sigma v_t - \sigma r_t^-)(X_t) dt \left. \right] \\ &+ \mathbb{E}_{X \sim \overrightarrow{\mathbb{P}}^{\nu, f+\sigma u}} \left[\int_0^T (u_t - r_t^+)(X_t) - (v_t - r_t^-)(X_t) \overrightarrow{dW}_t \right] \end{aligned} \quad (57)$$

and the last term vanishes because of (6). Therefore we see that there are 2 boundary terms, and 3 extra terms corresponding to the forward/backward process. By picking $\gamma^+, \gamma^- = 0$, and Lebesgue base measure for Γ_0, Γ_T , we get

$$D_{KL}(\overrightarrow{\mathbb{P}}^{\nu, f+\sigma u} \parallel \overleftarrow{\mathbb{P}}^{\mu, f+\sigma v}) = \mathbb{E}_{X \sim \overrightarrow{\mathbb{P}}^{\nu, f+\sigma u}} \left[\int_0^T \frac{1}{2} \|u_t(X_t) - v_t(X_t)\|^2 - \nabla \cdot (f_t + \sigma v_t)(X_t) dt \right] \quad (58)$$

$$+ \mathbb{E}_{X \sim \overrightarrow{\mathbb{P}}^{\nu, f+\sigma u}} \left[\log \frac{d\nu(X_0)}{d\mu(X_T)} + \int_0^T (u_t - v_t)(X_t) \overrightarrow{dW}_t \right] + \log Z \quad (59)$$

which agrees with Proposition 2.3 in (Richter et al., 2023) up to a conventional sign in v , and is also the same as the ELBO loss in (Chen et al., 2021a, Theorem 4).

Argument using Remark 1: Another way to show (53) is to start with Nelson's identity and apply Girsanov's theorem with (2) and time reversal of (3). Using the chain rule for the KL between two forward processes we get

$$\begin{aligned} D_{KL}(\overrightarrow{\mathbb{P}}^{\nu, f+\sigma u} \parallel \overleftarrow{\mathbb{P}}^{\mu, f+\sigma v}) &= \mathbb{E}_{\overrightarrow{\mathbb{P}}^{\nu, f+\sigma u}} \left[\log \left(\frac{d\overrightarrow{\mathbb{P}}^{\nu, f+\sigma u}}{d\overleftarrow{\mathbb{P}}^{\mu, f+\sigma v}} \right) (X) \right] \\ &= \mathbb{E}_{\overrightarrow{\mathbb{P}}^{\nu, f+\sigma u}} \left[\log \left(\frac{d\nu}{d\overleftarrow{\mathbb{P}}_0^{\mu, f+\sigma v}} \right) (X_0) + \frac{1}{2} \int_0^T \|u_t(X_t) - (v_t + \sigma \nabla \log \rho_t^{\mu, f+\sigma v})(X_t)\|^2 dt \right]. \end{aligned} \quad (60)$$

To see this is equivalent to (58)-(59), we use Fokker-Planck on the forward process with drift $v_t + \sigma \nabla \log \rho_t^{\mu, f+\sigma v}$ to reach

$$\begin{aligned} \mathbb{E}_{\overrightarrow{\mathbb{P}}^{\nu, f+\sigma u}} \left[\log \left(\frac{d\mu}{d\overleftarrow{\mathbb{P}}_0^{\mu, f+\sigma v}} \right) (X) - \log Z \right] &= \mathbb{E}_{\overrightarrow{\mathbb{P}}^{\nu, f+\sigma u}} \left[\log \left(\frac{d\overleftarrow{\mathbb{P}}_T^{\mu, f+\sigma v}}{d\overleftarrow{\mathbb{P}}_0^{\mu, f+\sigma v}} \right) (X) \right] \\ &= \mathbb{E}_{\overrightarrow{\mathbb{P}}^{\nu, f+\sigma u}} \left[\int_0^T -\nabla \cdot (f_t + \sigma v_t)(X_t) + \sigma (u_t - v_t)(X_t)^\top \nabla \log \rho_t^{\mu, f+\sigma v}(X_t) - \frac{\sigma^2}{2} \|\nabla \log \rho_t^{\mu, f+\sigma v}(X_t)\|^2 dt \right] \end{aligned} \quad (61)$$

as by Itô's lemma for the process (2) with drift $f + \sigma u$, (denote $\overleftarrow{\mathbb{P}}_t^{\mu, f+\sigma v}$ as ρ_t)

$$\begin{aligned} &\int_0^T \partial_t \log \overleftarrow{\mathbb{P}}_t^{\mu, f+\sigma v}(X_t^{f+\sigma u}) dt \\ &= \int_0^T \frac{1}{\rho_t} \left(-\nabla \cdot (\rho_t(f + \sigma v)) + \frac{\sigma^2}{2} \Delta \rho_t + \nabla \rho_t^\top (f + \sigma u) \right) dt + \sigma \int_0^T \frac{\nabla \rho_t^\top}{\rho_t} dW_t + \int_0^T \frac{\sigma^2}{2} \Delta \log \rho_t dt \\ &= \int_0^T -\frac{\nabla \rho_t^\top}{\rho_t} (f_t + \sigma v_t) + \frac{\sigma^2}{2} \nabla \log \rho_t - f_t - \sigma u_t - \nabla \cdot (f_t + \sigma v_t + \frac{\sigma^2}{2} \nabla \log \rho_t) + \frac{\sigma^2}{2} \Delta \log \rho_t dt + \int_0^T \sigma \frac{\nabla \rho_t^\top}{\rho_t} dW_t, \end{aligned}$$

which upon simple re-arranging and taking expectation over $X_t^{f+\sigma u} \sim \overrightarrow{\mathbb{P}}_t^{\nu, f+\sigma u}$ give (61). Now adding up the previous two displays (60) and (61) using

$$\mathbb{E}_{\overrightarrow{\mathbb{P}}^{\nu, f+\sigma u}} \left[\log \left(\frac{d\nu}{d\overleftarrow{\mathbb{P}}_0^{\mu, f+\sigma v}} \right) \right] = \mathbb{E}_{\overrightarrow{\mathbb{P}}^{\nu, f+\sigma u}} \left[\log \left(\frac{d\nu}{d\mu} \right) + \log \left(\frac{d\mu}{d\overleftarrow{\mathbb{P}}_0^{\mu, f+\sigma v}} \right) \right]$$

finishes the proof of the expression (53). The log-variance claim follows easily from this.

Reverse KL using Remark 1: Symmetrically, we can use Girsanov's theorem to compute the reverse KL divergence between two backward processes as:

$$\begin{aligned} D_{KL}(\overleftarrow{\mathbb{P}}^{\mu, f+\sigma v} \parallel \overrightarrow{\mathbb{P}}^{\nu, f+\sigma u}) &= \mathbb{E}_{\overleftarrow{\mathbb{P}}^{\mu, f+\sigma v}} \left[\log \left(\frac{d\overleftarrow{\mathbb{P}}^{\mu, f+\sigma v}}{d\overrightarrow{\mathbb{P}}^{\nu, f+\sigma u}} \right) (X) \right] \\ &= \mathbb{E}_{\overleftarrow{\mathbb{P}}^{\mu, f+\sigma v}} \left[\log \left(\frac{d\mu}{d\overrightarrow{\mathbb{P}}_T^{\nu, f+\sigma u}} \right) (X_T) + \frac{1}{2} \int_0^T \|v_t(X_t) - (u_t - \sigma \nabla \log \rho_t^{\nu, f+\sigma u})(X_t)\|^2 dt - \log Z \right]. \end{aligned}$$

We decompose

$$\mathbb{E}_{\overleftarrow{\mathbb{P}}^{\mu, f+\sigma v}} \left[\log \left(\frac{d\mu}{d\overrightarrow{\mathbb{P}}_T^{\nu, f+\sigma u}} \right) \right] = \mathbb{E}_{\overleftarrow{\mathbb{P}}^{\mu, f+\sigma v}} \left[\log \left(\frac{d\mu}{d\nu} \right) + \log \left(\frac{d\nu}{d\overrightarrow{\mathbb{P}}_T^{\nu, f+\sigma u}} \right) \right].$$

Now note the second term is nothing but $-\int_0^T \partial_t \log \overrightarrow{\mathbb{P}}_t^{\nu, f+\sigma u}(X_t) dt$ for $X_t \sim \overleftarrow{\mathbb{P}}^{\mu, f+\sigma v}$, and we compute using Fokker-Planck and backward Itô's lemma to reach (denote $\overrightarrow{\mathbb{P}}_t^{\nu, f+\sigma u}$ as ρ_t)

$$\begin{aligned} & \int_0^T \partial_t \log \overrightarrow{\mathbb{P}}_t^{\nu, f+\sigma u}(X_t^{f+\sigma v}) dt \\ &= \int_0^T \frac{1}{\rho_t} \left(-\nabla \cdot (\rho_t(f + \sigma u)) + \frac{\sigma^2}{2} \Delta \rho_t + \nabla \rho_t^\top (f + \sigma v) \right) dt + \sigma \int_0^T \frac{\nabla \rho_t^\top}{\rho_t} \overleftarrow{dW}_t - \int_0^T \frac{\sigma^2}{2} \Delta \log \rho_t dt \\ &= \int_0^T -\frac{\nabla \rho_t^\top}{\rho_t} (f_t + \sigma u_t - \frac{\sigma^2}{2} \nabla \log \rho_t - f_t - \sigma v_t) - \nabla \cdot (f_t + \sigma u_t - \frac{\sigma^2}{2} \nabla \log \rho_t) - \frac{\sigma^2}{2} \Delta \log \rho_t dt + \int_0^T \sigma \frac{\nabla \rho_t^\top}{\rho_t} \overleftarrow{dW}_t \\ &= \int_0^T \sigma (v_t - u_t) \nabla \log \rho_t + \frac{\sigma^2}{2} \|\nabla \log \rho_t\|^2 - \nabla \cdot (f_t + \sigma u_t) dt + \int_0^T \sigma \frac{\nabla \rho_t^\top}{\rho_t} \overleftarrow{dW}_t, \end{aligned}$$

which by using (7) and putting everything together allow us to finish. \square

Remark 12 (Explicit expression). In Proposition 1, up to constants, $D_{KL}(\overrightarrow{\mathbb{P}}^{\nu, f+\sigma^2 \nabla \phi} \| \overleftarrow{\mathbb{P}}^{\mu, f-\sigma^2 \nabla \psi})$ can be written as for $X \sim \overrightarrow{\mathbb{P}}^{\nu, f+\sigma^2 \nabla \phi}$,

$$\mathbb{E} \left[\int_0^T \frac{\sigma^2}{2} \|\nabla \phi_t(X_t) + \nabla \psi_t(X_t)\|^2 - \nabla \cdot (f_t - \sigma^2 \nabla \psi_t)(X_t) dt + \log \frac{\nu(X_0)}{\mu(X_T)} + \sigma \int_0^T (\nabla \phi_t + \nabla \psi_t)(X_t) \overrightarrow{dW}_t \right], \quad (62)$$

and the log-variance divergence between the same two path measures has $\text{Var}[\cdot]$ in place of $\mathbb{E}[\cdot]$. Moreover $D_{KL}(\overrightarrow{\mathbb{P}}^{\nu, f+\sigma^2 \nabla \phi} \| \overleftarrow{\mathbb{P}}^{\mu, f+\sigma^2 \nabla \phi_t - \sigma^2 \nabla \log \rho_t})$ evaluates to

$$\mathbb{E}_{\overrightarrow{\mathbb{P}}^{\nu, f+\sigma^2 \nabla \phi}} \left[\log \frac{\nu(X_0)}{\mu(X_T)} + \int_0^T \frac{\sigma^2}{2} \|\nabla \log \rho_t(X_t)\|^2 + \sigma^2 \nabla \cdot (\nabla \log \rho_t - \nabla \phi_t)(X_t) - \nabla \cdot f_t(X_t) dt \right]. \quad (63)$$

Both are straightforward consequences of Lemma 3.

Immediately follows is our main result: Proposition 1, along with Lemma 4 that sheds a different light on the losses (b) and (c) from Section 3.1.

Proof of Proposition 1. The first term in losses (a), (b), (d) involving D_{KL} can be written in terms of the (current) controls using Lemma 3, up to constants (c.f. (62)/(63)). One can regularize to enforce optimality while still ensuring the right marginals via

$$\mathcal{L}(\nabla \phi, \nabla \psi) := D_{KL}(\overrightarrow{\mathbb{P}}^{\nu, \sigma^2 \nabla \phi} \| \overleftarrow{\mathbb{P}}^{\mu, -\sigma^2 \nabla \psi}) + \lambda R(\nabla \psi) \quad \text{or} \quad D_{KL}(\overrightarrow{\mathbb{P}}^{\nu, \sigma^2 \nabla \phi} \| \overleftarrow{\mathbb{P}}^{\mu, -\sigma^2 \nabla \psi}) + \lambda' R'(\nabla \phi)$$

where $R(\cdot)$ can either utilize the variational formulation recast from (28) as in (a) or the optimality condition on the control as in (b). In both cases, the first term is a ρ constraint (time reversal consistency with correct terminal marginals), and the second one a control constraint (enforce optimality of trajectory).

For (b), we give one direction of the argument for $\nabla \psi$ first. Let $\overrightarrow{\mathbb{P}}^{\nu, f}$ denote the path measure associated with $dX_t = f_t(X_t)dt + \sigma dW_t$, $X_0 \sim \nu$, then $\overrightarrow{\mathbb{P}}^{\nu, f}$ almost surely, using Lemma 3, the Radon-Nikodym derivative between $\overrightarrow{\mathbb{P}}^{\nu, f}$ and the controlled backward process is

$$\log \left(\frac{d\overrightarrow{\mathbb{P}}^{\nu, f}}{d\overleftarrow{\mathbb{P}}^{\mu, f-\sigma^2 \nabla \psi_t}} \right) (X) = \log \frac{d\nu(X_0)}{d\mu(X_T)} + \int_0^T \frac{\sigma^2}{2} \|\nabla \psi_t\|^2 - \nabla \cdot (f - \sigma^2 \nabla \psi_t) dt + \sigma \int_0^T \nabla \psi_t^\top dW_t + \log Z.$$

In the case when the variance (taken along the prior $X \sim \overrightarrow{\mathbb{P}}^{\nu, f}$)

$$\text{Var} \left(\psi_T(X_T) - \psi_0(X_0) - \int_0^T \frac{\sigma^2}{2} \|\nabla \psi_t\|^2 + \nabla \cdot f - \sigma^2 \Delta \psi_t(X_t) dt - \int_0^T \sigma \nabla \psi_t^\top dW_t \right) = 0,$$

it implies that the random quantity is almost surely a constant independent of the realization, and

$$\log \left(\frac{d\overrightarrow{\mathbb{P}}^{\nu, f}}{d\overleftarrow{\mathbb{P}}^{\mu, f-\sigma^2 \nabla \psi_t}} \right) (X) = \underbrace{\log \nu(X_0) - \psi_0(X_0)}_{-f(X_0)} + \underbrace{\psi_T(X_T) - \log \mu(X_T) + \log Z}_{-g(X_T)}.$$

Recall the terminal constraint $\overrightarrow{\mathbb{P}}_0^{\nu, f + \sigma^2 \nabla \phi_t} = \overleftarrow{\mathbb{P}}_0^{\mu, f - \sigma^2 \nabla \psi_t} = \nu$ and $\overrightarrow{\mathbb{P}}_T^{\nu, f + \sigma^2 \nabla \phi_t} = \overleftarrow{\mathbb{P}}_T^{\mu, f - \sigma^2 \nabla \psi_t} = \mu$ are imposed by the first KL term, therefore using Nelson's identity $-\nabla \psi_0(X_0) = \nabla \phi_0(X_0) - \nabla \log \nu(X_0)$ and $-\nabla \psi_T(X_T) = \nabla \phi_T(X_T) - \nabla \log p_{\text{target}}(X_T)$, from which we can deduce that the factorization property (47) holds and concludes that $\overleftarrow{\mathbb{P}}^{\mu, f - \sigma^2 \nabla \psi_t}$ must be the unique solution to the SB problem. The other direction on $\nabla \phi$ is largely similar, and one can show using Girsanov's theorem and the variance condition that along the prior $X \sim \overrightarrow{\mathbb{P}}^{\nu, f}$,

$$\log \left(\frac{d\overrightarrow{\mathbb{P}}^{\nu, f + \sigma^2 \nabla \phi_t}}{d\overrightarrow{\mathbb{P}}^{\nu, f}} \right) (X) = \int_0^T -\frac{\sigma^2}{2} \|\nabla \phi_t\|^2 dt + \int_0^T \sigma \nabla \phi_t^\top dW_t = \underbrace{\phi_T(X_T)}_{g(X_T)} - \underbrace{\phi_0(X_0)}_{f(X_0)}.$$

This allows us to conclude that the factorization characterization (47) holds in the same way. Note that evaluating the variance regularizer only requires simulating from the reference process (14).

In (c), the first two parts enforce

$$\phi_T(X_T) + \psi_T(X_T) = \log p_{\text{target}}(X_T) \quad \text{and} \quad \phi_0(X_0) + \psi_0(X_0) = \log p_{\text{prior}}(X_0) = \log \nu(X_0).$$

Now for any ϕ_t , the likelihood ratio along $dX_t = (f + \sigma^2 \nabla \phi_t)dt + \sigma dW_t$, $X_0 \sim \nu$ is

$$\log \left(\frac{d\overrightarrow{\mathbb{P}}^{\nu, f + \sigma^2 \nabla \phi_t}}{d\overrightarrow{\mathbb{P}}^{\nu, f}} \right) (X) = \int_0^T \frac{\sigma^2}{2} \|\nabla \phi_t\|^2 dt + \int_0^T \sigma \nabla \phi_t^\top dW_t, \quad (64)$$

which according to (47), has to be equal to

$$\psi_0(X_0) + \phi_T(X_T) - \log \nu(X_0) = -\phi_0(X_0) + \phi_T(X_T) \quad \mathbb{P}^{\nu, f} \text{ a.s.} \Rightarrow \mathbb{P}^{\nu, f + \sigma^2 \nabla \phi} \text{ a.s.}$$

for $\nabla \phi$ to be optimal, justifying

$$\text{Var}_{X \sim \overrightarrow{\mathbb{P}}^{\nu, f + \sigma^2 \nabla \phi}} \left(\phi_T(X_T) - \phi_0(X_0) - \frac{\sigma^2}{2} \int_0^T \|\nabla \phi_t\|^2(X_t) dt - \sigma \int_0^T \nabla \phi_t(X_t)^\top dW_t \right).$$

In a similar spirit, using (55)-(56) and (8), for any ψ_t , along the same process $X \sim \overrightarrow{\mathbb{P}}^{\nu, f + \sigma^2 \nabla \phi_t}$,

$$\begin{aligned} \log \left(\frac{d\overrightarrow{\mathbb{P}}^{\nu, f}}{d\overleftarrow{\mathbb{P}}^{\mu, f - \sigma^2 \nabla \psi_t}} \right) (X) &= \int_0^T \sigma^2 \nabla \psi_t^\top \nabla \phi_t + \frac{\sigma^2}{2} \|\nabla \psi_t\|^2 - \nabla \cdot (f_t - \sigma^2 \nabla \psi_t) dt + \int_0^T \sigma \nabla \psi_t^\top dW_t \\ &+ \log \left(\frac{d\nu(X_0)}{d\mu(X_T)} \right) + \log Z, \end{aligned} \quad (65)$$

which again using (47), has to be equal to

$$-\psi_0(X_0) - \phi_T(X_T) + \log \nu(X_0) = \log \nu(X_0) - \psi_0(X_0) + \psi_T(X_T) - \log p_{\text{target}}(X_T)$$

for $\nabla \psi$ to be optimal, yielding the claimed variance regularizer. Additionally, in order to verify the terminal constraint at $0, T$ along $\overrightarrow{\mathbb{P}}^{\nu, f + \sigma^2 \nabla \phi_t}$, it suffices to sum up (64)-(65), which due to the first 2 terms of the loss, gives

$$-\phi_0(X_0) + \phi_T(X_T) - \psi_0(X_0) - \log p_{\text{target}}(X_T) + \psi_T(X_T) + \log \nu(X_0) = 0.$$

This necessarily imposes the time-reversal consistency $\overrightarrow{\mathbb{P}}^{\nu, f + \sigma^2 \nabla \phi_t} / \overleftarrow{\mathbb{P}}^{\mu, f - \sigma^2 \nabla \psi_t} = 1$ a.s. for the LHS.

In (d), we use $\nabla \phi_t$ and $\nabla \log \rho_t$ as optimization variables instead of the two drifts, and it follows from the dynamical formulation (35)-(36). The first part establishes a particular relationship between the two variables (namely $\nabla \phi_t$ traces out a curve of measures ρ_t), and the second part enforces optimality among all curves transporting between ν and μ . \square

It is important to note that the dynamics for ϕ_t, ψ_t below are adapted to the same filtration generated by the Brownian motion corresponding to $X_t \sim \overrightarrow{\mathbb{P}}$, i.e., ϕ_t, ψ_t are interpreted as functions of X_t, t . They are not time-reversed SDE, but rather terminal-constrained SDEs.

Lemma 4 (SDE correspondence to SB optimality). *We have for the optimal forward drift $\nabla\phi_t$ and $X \sim \overrightarrow{\mathbb{P}}^{\nu, f}$ as in (14),*

$$d\phi_t(X_t) = -\frac{\sigma^2}{2}\|\nabla\phi_t(X_t)\|^2 dt + \sigma\nabla\phi_t(X_t)^\top d\overrightarrow{W}_t,$$

analogously for the optimal backward drift $-\nabla\psi_t$, along $X \sim \overrightarrow{\mathbb{P}}^{\nu, f}$,

$$d\psi_t(X_t) = \left[\frac{\sigma^2}{2}\|\nabla\psi_t\|^2 - \nabla \cdot f_t + \sigma^2\Delta\psi_t \right](X_t)dt + \sigma\nabla\psi_t(X_t)^\top d\overrightarrow{W}_t.$$

Moreover, along the controlled forward dynamics $X \sim \overrightarrow{\mathbb{P}}^{\nu, f + \sigma^2\nabla\phi}$, the optimal control ϕ, ψ satisfy

$$d\phi_t(X_t) = \frac{\sigma^2}{2}\|\nabla\phi_t(X_t)\|^2 dt + \sigma\nabla\phi_t(X_t)^\top d\overrightarrow{W}_t, \quad (66)$$

$$d\psi_t(X_t) = \left[\frac{\sigma^2}{2}\|\nabla\psi_t\|^2 + \nabla \cdot (\sigma^2\nabla\psi_t - f_t) + \sigma^2\nabla\phi_t^\top\nabla\psi_t \right](X_t)dt + \sigma\nabla\psi_t(X_t)^\top d\overrightarrow{W}_t. \quad (67)$$

In the above, $\nabla\phi_t, \nabla\psi_t$ refer to the optimal forward / backward drift in the SDE

$$dX_t = [f_t(X_t) + \sigma^2\nabla\phi_t(X_t)]dt + \sigma d\overrightarrow{W}_t, \quad X_0 \sim \nu,$$

$$dX_t = [f_t(X_t) - \sigma^2\nabla\psi_t(X_t)]dt + \sigma d\overleftarrow{W}_t, \quad X_T \sim \mu,$$

and $\phi_T(X_T) + \psi_T(X_T) = \log p_{\text{target}}(X_T)$, $\phi_0(X_0) + \psi_0(X_0) = \log \nu(X_0)$ for $X \sim \overrightarrow{\mathbb{P}}^{\nu, f + \sigma^2\nabla\phi}$.

Proof of Lemma 4. Using Itô's lemma, we have along the reference SDE $dX_t = f_t(X_t)dt + \sigma dW_t$, $X_0 \sim \nu$,

$$d\phi_t = \left[\frac{\partial\phi_t}{\partial t} + \nabla\phi_t^\top f_t + \frac{\sigma^2}{2}\Delta\phi_t \right] dt + \sigma\nabla\phi_t^\top d\overrightarrow{W}_t.$$

Now deducing from (41), since the optimal ϕ_t solves the PDE for all $(t, x) \in [0, T] \times \mathbb{R}^d$

$$\partial_t\phi_t = -f_t^\top\nabla\phi_t - \frac{\sigma^2}{2}\Delta\phi_t - \frac{\sigma^2}{2}\|\nabla\phi_t\|^2,$$

substituting the last display into the previous one gives the result. Analogously, along the same reference process with Itô's lemma,

$$d\psi_t = \left[\frac{\partial\psi_t}{\partial t} + \nabla\psi_t^\top f_t + \frac{\sigma^2}{2}\Delta\psi_t \right] dt + \sigma\nabla\psi_t^\top d\overrightarrow{W}_t$$

and using the fact (41) that the optimal ψ_t solves for all $(t, x) \in [0, T] \times \mathbb{R}^d$

$$\partial_t\psi_t = -\nabla\psi_t^\top f_t - \nabla \cdot f_t + \frac{\sigma^2}{2}(\|\nabla\psi_t\|^2 + \Delta\psi_t)$$

and plugging into the previous display yields the claim. In both of the PDE derivations above, we used the fact that for any $g: \mathbb{R}^d \rightarrow \mathbb{R}$,

$$\frac{1}{g}\nabla^2 g = \nabla^2 \log g + \frac{1}{g^2}\nabla g \nabla g^\top \Rightarrow \frac{1}{g}\Delta g = \Delta \log g + \|\nabla \log g\|^2 \quad (68)$$

by taking trace on both sides.

The second part of the lemma statement, where X_t evolves along the optimally controlled SDE, follows from (Chen et al., 2021a, Theorem 3) up to a change of variable. Notice the sign change and the absence of the cross term in the dynamics for ϕ_t, ψ_t when $X \sim \overrightarrow{\mathbb{P}}^{\nu, f}$ vs. $X \sim \overrightarrow{\mathbb{P}}^{\nu, f + \sigma^2\nabla\phi}$. \square

Remark 13 (Equivalence between SDE, PDE, Path measure). Adding (66)-(67) up and integrating over time, we get that along the *optimally controlled* forward trajectory,

$$\log p_{\text{target}}(X_T) - \log \nu(X_0) = \int_0^T \frac{\sigma^2}{2}\|\nabla\phi_t(X_t) + \nabla\psi_t(X_t)\|^2 + \nabla \cdot (\sigma^2\nabla\psi_t - f_t)(X_t)dt + \sigma \int_0^T (\nabla\phi_t + \nabla\psi_t)(X_t)^\top d\overrightarrow{W}_t,$$

exactly matching the KL objective (62) $D_{KL}(\overrightarrow{\mathbb{P}}^{\nu, f + \sigma^2 \nabla \phi} \parallel \overleftarrow{\mathbb{P}}^{\mu, f - \sigma^2 \nabla \psi}) = 0$. This implies that the optimally controlled dynamics is one solution that satisfy the $\nu - \mu$ marginal. The summation of ϕ_t, ψ_t , however, introduces ambiguity/non-uniqueness as any $+C$ shift in one of ϕ, ψ that's cancelled by $-C$ in another will result in the same integral equality for $\partial_t \log \rho_t(X_t)$. What we really want is therefore conditions on $\log\left(\frac{d\overrightarrow{\mathbb{P}}^{\nu, f + \sigma^2 \nabla \phi}}{d\overrightarrow{\mathbb{P}}^{\nu, f}}\right)$ and $\log\left(\frac{d\overleftarrow{\mathbb{P}}^{\mu, f}}{d\overleftarrow{\mathbb{P}}^{\mu, f - \sigma^2 \nabla \psi}}\right)$ separately instead of $\log\left(\frac{d\overrightarrow{\mathbb{P}}^{\nu, f + \sigma^2 \nabla \phi}}{d\overleftarrow{\mathbb{P}}^{\mu, f - \sigma^2 \nabla \psi}}\right)$ only. An equivalent PDE representation of $\partial_t \log \rho_t(X_t)$ can be written as

$$\begin{aligned} \partial_t \log \rho_t(X_t) &= \frac{1}{\rho_t} (\partial_t \rho_t + \nabla \rho_t^\top \dot{X}_t) \\ &= \frac{1}{\rho_t} [-\nabla \cdot (\rho_t (f_t + \sigma^2 \nabla \phi_t)) + \frac{\sigma^2}{2} \Delta \rho_t] + \frac{1}{\rho_t} \nabla \rho_t^\top (f_t + \sigma^2 \nabla \phi_t - \frac{\sigma^2}{2} \nabla \log \rho_t) \\ &= -\sigma^2 \Delta \phi_t - \nabla \cdot f_t + \frac{\sigma^2}{2} \frac{1}{\rho_t} \Delta \rho_t - \frac{\sigma^2}{2} \|\nabla \log \rho_t\|^2 = -\sigma^2 \Delta \phi_t - \nabla \cdot f_t + \frac{\sigma^2}{2} \Delta \log \rho_t. \end{aligned} \quad (69)$$

Proposition 2 and Lemma 1 are stated in Section 3.2, whose proof we give below.

Proof of Proposition 2. The optimal $\nabla \phi_t, \nabla \psi_t$ allow us to calculate $\log Z$ for p_{target} using (62) as (can be used without expectation, or with expectation and ignore the last zero-mean martingale term)

$$\begin{aligned} \log Z &= \mathbb{E}_{\overrightarrow{\mathbb{P}}^{\nu, f + \sigma^2 \nabla \phi}} \left[-\frac{\sigma^2}{2} \int_0^T \|\nabla \phi_t(X_t) + \nabla \psi_t(X_t)\|^2 dt + \int_0^T \nabla \cdot (f_t(X_t) - \sigma^2 \nabla \psi_t(X_t)) dt - \log \frac{d\nu(X_0)}{d\mu(X_T)} \right] \\ &\quad + \mathbb{E}_{\overrightarrow{\mathbb{P}}^{\nu, f + \sigma^2 \nabla \phi}} \left[-\sigma \int_0^T (\nabla \phi_t + \nabla \psi_t)(X_t) d\overrightarrow{W}_t \right] =: \mathbb{E}[-S]. \end{aligned}$$

Alternatively using (49), with the optimal $\nabla \phi^*, \nabla \psi^*$, since Z is independent of X_T ,

$$-\log Z = \log \nu(X_0) - \frac{\sigma^2}{2} \int_0^T \nabla \cdot (\nabla \log \phi_t^* - \nabla \log \psi_t^*)(X_t) dt - \int_0^T \nabla \cdot f_t(X_t) dt - \log \mu(X_T), \quad (70)$$

in which case the estimator is exact with X_t following (48).

In general for imperfect control, since $D_{KL}(\overrightarrow{\mathbb{P}}^{\nu, f + \sigma^2 \nabla \phi} \parallel \overleftarrow{\mathbb{P}}^{\mu, f - \sigma^2 \nabla \psi}) > 0$, $\log Z$ will only be lower bounded by $\mathbb{E}[-S]$. Using Lemma 3 however,

$$\begin{aligned} 1 &= \mathbb{E}_{\overrightarrow{\mathbb{P}}^{\nu, f + \sigma^2 \nabla \phi}} \left[\left(\frac{d\overrightarrow{\mathbb{P}}^{\nu, f + \sigma^2 \nabla \phi}}{d\overleftarrow{\mathbb{P}}^{\mu, f - \sigma^2 \nabla \psi}} \right)^{-1} \right] \\ &= \mathbb{E}_{\overrightarrow{\mathbb{P}}^{\nu, f + \sigma^2 \nabla \phi}} \left[\exp \left(-\frac{\sigma^2}{2} \int_0^T \|\nabla \phi_t + \nabla \psi_t\|^2 + \nabla \cdot (f_t - \sigma^2 \nabla \psi_t) dt - \sigma \int_0^T (\nabla \phi_t + \nabla \psi_t) dW_t - \log \frac{\nu}{\mu} \right) \frac{1}{Z} \right] \\ &=: \mathbb{E}[\exp(-S')/Z], \end{aligned} \quad (71)$$

giving $Z = \mathbb{E}_{\overrightarrow{\mathbb{P}}^{\nu, f + \sigma^2 \nabla \phi}}[\exp(-S')]$ as unbiased estimator using any (potentially sub-optimal) controls $\nabla \phi, \nabla \psi$.

For the importance sampling, we use path weights suggested by the terminal requirement that $X_T^{\phi^*} \sim \mu$, therefore using (69) the path weight becomes

$$\begin{aligned} w^\phi(X_T^\phi) &= \frac{d\mu}{d\mathbb{P}_{X_T^\phi}}(X_T^\phi) = \frac{d\mu(X_T^\phi)}{d\nu(X_0^\phi)} \frac{d\nu(X_0^\phi)}{d\mathbb{P}_{X_T^\phi}(X_T^\phi)} \\ &= \frac{d\mu(X_T^\phi)}{d\nu(X_0^\phi)} \exp \left(-\int_0^T \partial_t \log \rho_t^\phi(X_t^\phi) dt \right) \\ &= \frac{d\mu(X_T^\phi)}{d\nu(X_0^\phi)} \exp \left(\int_0^T \sigma^2 \Delta \phi_t - \frac{\sigma^2}{2} \Delta \log \rho_t^\phi + \nabla \cdot f_t dt \right). \end{aligned}$$

Indeed, this choice guarantees $\mathbb{E}_\phi[g(X_T^\phi)w^\phi(X_T^\phi)] = \int g(x)\mu(x)dx$ for any function g on the terminal variable X_T generated with the suboptimal control ϕ . It remains to normalize the weights (i.e., account for the constant Z) via dividing by $\mathbb{E}_\phi[w^\phi(X_T^\phi)] = Z$. In the case of perfect controls, all samples will have equal weight. \square

Remark 14 (optimal control \Leftrightarrow optimal estimator). In general one always has the importance sampling identity

$$1 = \mathbb{E}_{\overrightarrow{\mathbb{P}}^{\nu, f + \sigma^2 \nabla \phi}} \left[\left(\frac{d\overrightarrow{\mathbb{P}}^{\nu, f + \sigma^2 \nabla \phi}}{d\overleftarrow{\mathbb{P}}^{\mu, f - \sigma^2 \nabla \psi}} \right)^{-1} \right].$$

With the optimal controls ϕ^*, ψ^* , we see that since inside the square bracket of (71), we have $\exp(0) = 1$ holds deterministically (although the path is random), the Z -estimator is optimal when optimally controlled in the sense that it's unbiased and has zero variance (it is almost surely a constant and equality holds not only in expectation). This property is desirable for the Monte-Carlo estimates that we employ. Such optimal control \Leftrightarrow optimal sampling equivalence also appears in (Thijssen and Kappen, 2015) for path integral control problem that involves a *single control*. This choice of ϕ^*, ψ^* also admits the interpretation of minimizing the χ^2 -divergence between path measures:

$$\chi^2(\overleftarrow{\mathbb{P}}^{\mu, f - \sigma^2 \nabla \psi} \| d\overrightarrow{\mathbb{P}}^{\nu, f + \sigma^2 \nabla \phi}) = \text{Var}_{\overrightarrow{\mathbb{P}}^{\nu, f + \sigma^2 \nabla \phi}} \left[\frac{\overleftarrow{\mathbb{P}}^{\mu, f - \sigma^2 \nabla \psi}}{\overrightarrow{\mathbb{P}}^{\nu, f + \sigma^2 \nabla \phi}} \right].$$

Proof of Lemma 1. We obtain the forward trajectory

$$X_{k+1}^i = X_k^i + (f_k(X_k^i) + \sigma^2 \nabla \phi_k(X_k^i))h + \sigma \sqrt{h} \cdot z_k^i, \quad z_k^i \sim \mathcal{N}(0, I) \quad (72)$$

with Euler-Maruyama for each of the $i \in [N]$ samples. Rewriting the term (65) using (8), (55)-(56) and proceeding with the approximation (4)-(5) give

$$\begin{aligned} & \log \frac{\nu(X_0)}{p_{\text{target}}(X_T)} + \frac{1}{\sigma^2} \int_0^T f_t(X_t) d\overrightarrow{X}_t - \frac{1}{2\sigma^2} \int_0^T \|f_t(X_t)\|^2 dt - \frac{1}{\sigma^2} \int_0^T (f_t - \sigma^2 \nabla \psi_t)(X_t) d\overleftarrow{X}_t + \frac{1}{2\sigma^2} \int_0^T \|(f_t - \sigma^2 \nabla \psi_t)(X_t)\|^2 dt \\ & \approx \frac{1}{\sigma^2} \sum_{k=0}^{K-1} f_k(X_k)^\top (X_{k+1} - X_k) - \frac{1}{2\sigma^2} \|f_k(X_k)\|^2 h \\ & - \frac{1}{\sigma^2} (f_{k+1}(X_{k+1}) - \sigma^2 \nabla \psi_{k+1}(X_{k+1}))(X_{k+1} - X_k) + \frac{1}{2\sigma^2} \|f_{k+1}(X_{k+1}) - \sigma^2 \nabla \psi_{k+1}(X_{k+1})\|^2 h + \log \frac{\nu(X_0)}{p_{\text{target}}(X_T)} \\ & = \sum_{k=0}^{K-1} \frac{1}{2\sigma^2 h} \|X_k - X_{k+1} + (f_{k+1} - \sigma^2 \nabla \psi_{k+1})(X_{k+1})h\|^2 - \sum_{k=0}^{K-1} \frac{1}{2\sigma^2 h} \|X_{k+1} - X_k - f_k(X_k)h\|^2 + \log \frac{\nu(X_0)}{p_{\text{target}}(X_T)} \\ & \stackrel{!}{=} \log \nu(X_0) - \psi_0(X_0) + \psi_T(X_T) - \log p_{\text{target}}(X_T) \end{aligned}$$

which yields the estimator for the variance regularizer on ψ when $(X_k)_k$ follows (72). Note that compared to a naive discretization of the RHS of (65), we are able to avoid any divergence and stochastic terms.

It is also possible to avoid the divergence term in (71) by leveraging similar ideas. Direct computation using (55)-(56) on $\frac{d\overleftarrow{\mathbb{P}}^{\mu, f - \sigma^2 \nabla \psi}}{d\overrightarrow{\mathbb{P}}^{\nu, f + \sigma^2 \nabla \phi}}$ tells us the normalizing constant estimator

$$Z \approx \frac{1}{N} \sum_{i=1}^N \exp \left(\log \frac{\mu}{\nu} - \sum_{k=0}^{K-1} \frac{1}{2\sigma^2 h} \|X_k^i - X_{k+1}^i + (f_{k+1} - \sigma^2 \nabla \psi_{k+1})(X_{k+1}^i)h\|^2 + \frac{1}{2} \|z_k^i\|^2 \right)$$

for the same Euler-Maruyama trajectory (72), where we used that the additional term

$$\sum_{k=0}^{K-1} \frac{1}{2\sigma^2 h} \|X_{k+1} - X_k - (f_k + \sigma^2 \nabla \phi_k)(X_k)h\|^2 = \frac{1}{2} \sum_{k=0}^{K-1} \|z_k\|^2$$

from the update (72). \square

E MISSING AUXILIARY RESULTS

Remark 15 (Backward drift). For PINN (20), a regularizer on the backward drift involving $\nabla\psi$ is also possible and will be:

$$(19) + \lambda \cdot \frac{h}{n} \sum_{i=1}^n \sum_{k=0}^K \left| \partial_t \psi(x_k^i, kh) - \frac{\sigma^2}{2} [\Delta \psi(x_k^i, kh) - \|\nabla \psi(x_k^i, kh)\|^2] \right|. \quad (73)$$

And similarly for variance loss (22), which will read as

$$(19) + \frac{\lambda}{K+1} \cdot \text{Var}_n \left[\psi(y_{K+1}^i, (K+1)h) - \psi(y_0^i, 0) + \sum_{k=0}^K \frac{1}{2\sigma^2 h} \left(\|y_{k+1}^i - y_k^i\|^2 - \|y_k^i - y_{k+1}^i - \sigma^2 h \nabla \psi(y_{k+1}^i, (k+1)h)\|^2 \right) \right] \quad (74)$$

and TD loss (24) becomes

$$(19) + \lambda \cdot \frac{1}{n} \sum_{i=1}^n \sum_{k=0}^K h \cdot \left| \psi(y_{k+1}^i, (k+1)h) - \psi(y_k^i, kh) - \frac{\sigma^2 h}{2} \|\nabla \psi(y_k^i, kh)\|^2 - \sigma^2 \Delta \psi(y_k^i, kh) - \sigma \sqrt{h} \nabla \psi(y_k^i, kh)^\top Z_k^i \right|. \quad (75)$$

However, these should witness similar behavior as the regularizer on the forward control $\nabla\phi$ that we experimented with (using the same trajectories). Note crucially there is no divergence term in (74) in contrast to (75), (73).

Lastly we mention a word about contraction for method (12).

Remark 16 (Contraction). In Section 2.2 we claimed that for two processes $(p_t)_t, (q_t)_t$ with different initial-ization, but same drift $\sigma v + \sigma^2 s$ where s is the score function, $\partial_t D_{KL}(p_t \| q_t) = -\sigma^2/2 \cdot \mathbb{E}_{p_t} [\|\nabla \log \frac{p_t}{q_t}\|^2] \leq 0$ contracts towards each other, when we run the generative process

$$dX_t = [\sigma v_t(X_t) + \sigma^2 s_t(X_t)] dt + \sigma d\overrightarrow{W}_t, \quad X_0 \sim \nu \neq \overleftarrow{\mathbb{P}}_0^{\mu, \sigma v},$$

although the actual rate may be slow. We give this short calculation here for completeness:

$$\begin{aligned} & \partial_t D_{KL}(p_t \| q_t) \\ &= \int (\partial_t p_t(x)) \log \frac{p_t(x)}{q_t(x)} dx + \int q_t(x) \left[\frac{\partial_t p_t(x)}{q_t(x)} - \frac{p_t(x) \partial_t q_t(x)}{q_t^2(x)} \right] dx \\ &= \int p_t \left[\sigma v_t + \sigma^2 s_t - \frac{\sigma^2}{2} \nabla \log p_t(x) \right]^\top \nabla \log \frac{p_t(x)}{q_t(x)} dx - \int \frac{p_t(x)}{q_t(x)} \partial_t q_t(x) dx \\ &= \int p_t \left[\sigma v_t + \sigma^2 s_t - \frac{\sigma^2}{2} \nabla \log p_t(x) \right]^\top \nabla \log \frac{p_t(x)}{q_t(x)} dx - \int \nabla \frac{p_t(x)}{q_t(x)} \left[\sigma v_t + \sigma^2 s_t - \frac{\sigma^2}{2} \nabla \log q_t(x) \right] q_t(x) dx \\ &= \int \left[\sigma v_t + \sigma^2 s_t - \frac{\sigma^2}{2} \nabla \log p_t(x) - \sigma v_t - \sigma^2 s_t + \frac{\sigma^2}{2} \nabla \log q_t(x) \right]^\top \nabla \log \frac{p_t(x)}{q_t(x)} \cdot p_t(x) dx \\ &= -\frac{\sigma^2}{2} \int \left\| \nabla \log \frac{p_t(x)}{q_t(x)} \right\|^2 p_t(x) dx \leq 0. \end{aligned}$$

F SECOND-ORDER DYNAMICS

The motivation of this section is to design a smoother trajectory for X_t while still maintaining optimality (and therefore uniqueness) of the dynamics. Suppose the reference Q is given by the following augmented process with a velocity variable $V_t \in \mathbb{R}^d$, and (X_t, V_t) have as the stationary distribution $\mathcal{N}(0, I) \otimes \mathcal{N}(0, I)$:

$$dX_t = V_t dt \quad (76)$$

$$dV_t = -X_t dt - \gamma V_t dt + \sqrt{2\gamma} d\overrightarrow{W}_t \quad (77)$$

We assume it is initialized at $Z_0 := (X_0, V_0) \sim \nu \otimes \mathcal{N}(0, I)$ independent and would like to enforce $Z_T := (X_T, V_T) \sim \mu \otimes \mathcal{N}(0, I)$ at the terminal. In this second-order case (Dockhorn et al., 2022), to solve the optimal trajectory problem, we formulate P as the controlled process

$$\inf_{\rho, u} \int_{\mathbb{R}^{2d}} \int_0^T \gamma \|u_t(Z_t)\|^2 \rho_t(Z_t) dt dz \quad (78)$$

$$\text{s.t. } dX_t = V_t dt \quad (79)$$

$$dV_t = -[X_t + 2\gamma u_t(Z_t)]dt - \gamma V_t dt + \sqrt{2\gamma} d\overrightarrow{W}_t, \rho_0(Z_0) = \nu \otimes \mathcal{N}(0, I), \rho_T(Z_T) = \mu \otimes \mathcal{N}(0, I) \quad (80)$$

One could check via the Girsanov's theorem that by picking

$$\bar{b}_t = \begin{bmatrix} V_t \\ -X_t - \gamma V_t \end{bmatrix}, \quad b_t = \begin{bmatrix} V_t \\ -X_t - 2\gamma u_t(Z_t) - \gamma V_t \end{bmatrix}, \quad G_t = \begin{bmatrix} 0 & 0 \\ 0 & \sqrt{2\gamma} I \end{bmatrix}$$

since $\bar{b}_t - b_t \in \text{image}(G_t)$, the KL divergence between the two path measures P and Q is $\mathbb{E}[\int_0^T \gamma \|u_t(Z_t)\|^2 dt]$. This is the SB goal of

$$\min_{P_0 \sim \nu \otimes \mathcal{N}, P_T \sim \mu \otimes \mathcal{N}} D_{KL}(P \| Q),$$

which if minimized will identify the path with the minimum control effort between the two time marginals. We note that this formulation is different from the one in (Chen et al., 2023, Section 3), and is closer to an underdamped version of the SB dynamics. We denote the corresponding controlled path measure (79)-(80) as $\overrightarrow{\mathbb{P}}$.

The Radon-Nikodym likelihood ratio from Lemma 3 still applies, therefore to impose path measure consistency, we introduce a backward control $o(Z_t, t)$ for the process $\overleftarrow{\mathbb{P}}$:

$$dX_t = V_t dt \quad (81)$$

$$dV_t = -[X_t - 2\gamma o_t(Z_t)]dt - \gamma V_t dt + \sqrt{2\gamma} \overleftarrow{dW}_t. \quad (82)$$

The KL divergence $D_{KL}(\overrightarrow{\mathbb{P}} \| \overleftarrow{\mathbb{P}})$ for the augmented process becomes (from now on we will take $\gamma = 2$ for simplicity corresponding to critical damping)

$$\mathbb{E}_{Z \sim \overrightarrow{\mathbb{P}}} \left[\int_0^T 2 \|u_t(Z_t) + o_t(Z_t)\|^2 - \nabla \cdot \hat{b}_t(Z_t) dt + \log \frac{\nu(X_0) \otimes \mathcal{N}(V_0)}{\mu(X_T) \otimes \mathcal{N}(V_T)} \right] + C \quad (83)$$

for $\gamma = 2$ and

$$\hat{b}_t = \begin{bmatrix} V_t \\ -X_t + 2\gamma o_t(Z_t) - \gamma V_t \end{bmatrix},$$

with $\nabla \cdot \hat{b}_t(Z_t) = -\gamma d + 2\gamma \text{div}_V(o_t(Z_t))$. We minimize over vector fields $u(Z_t, t), o(Z_t, t)$ taking gradient forms to impose time reversal consistency. Below we derive a corresponding PINN and a variance regularizer for this dynamics, first on the forward drift followed by the backward drift.

Forward condition Writing out the optimality condition for the optimization problem (78), we have for a Lagrange multiplier $\lambda(Z_t, t)$, since by continuity equation the dynamics (79)-(80) can be rewritten as

$$\partial_t \rho_t(Z_t) + \nabla_{[X, V]} \cdot \left(\rho_t(Z_t) \begin{bmatrix} V_t \\ -X_t - 4u_t(Z_t) - 2V_t - 2\nabla_V \log \rho_t(Z_t) \end{bmatrix} \right) = 0, \quad (84)$$

we seek to optimize the Lagrangian

$$\int_{\mathbb{R}^{2d}} \int_0^T 2 \|u_t(Z_t)\|^2 \rho_t(Z_t) + \lambda(Z_t, t) \left[\partial_t \rho + \nabla_{[X, V]} \cdot \left(\rho_t(Z_t) \begin{bmatrix} V_t \\ -X_t - 4u_t(Z_t) - 2V_t - 2\nabla_V \log \rho_t(Z_t) \end{bmatrix} \right) \right] dt dz.$$

Performing integration by parts, we have

$$\int_{\mathbb{R}^{2d}} \int_0^T \left\{ 2 \|u_t(Z_t)\|^2 - \partial_t \lambda(Z_t, t) - \nabla_{[X, V]} \lambda(Z_t, t)^\top \begin{bmatrix} V_t \\ -X_t - 4u_t(Z_t) - 2V_t \end{bmatrix} - 2\Delta_V \lambda(Z_t, t) \right\} \rho_t(Z_t) dt dz.$$

Fixing ρ , the optimal control $u_t \in \mathbb{R}^d$ satisfies

$$u_t(Z_t) = -\nabla_V \lambda(Z_t, t). \quad (85)$$

Plugging this choice back in, the optimal $\lambda(Z_t, t)$ must satisfies the following PDE:

$$\begin{aligned} 2\|\nabla_V \lambda(Z_t, t)\|^2 - \partial_t \lambda(Z_t, t) - \nabla_X \lambda(Z_t, t)^\top V_t + \nabla_V \lambda(Z_t, t)^\top (X_t - 4\nabla_V \lambda(Z_t, t) + 2V_t) - 2\Delta_V \lambda(Z_t, t) &= 0 \\ \Rightarrow \partial_t \lambda(Z_t, t) &= -2\|\nabla_V \lambda(Z_t, t)\|^2 - \nabla_{[X, V]} \lambda(Z_t, t)^\top \bar{b}_t - 2\Delta_V \lambda(Z_t, t) \end{aligned} \quad (86)$$

where the $\Delta_V \lambda(Z_t, t)$ term is interpreted as $\text{Trace}(\nabla_V^2 \lambda(Z_t, t))$. Turning to the variance loss, use Itô's lemma we get that along the reference SDE (76)-(77),

$$d\lambda_t(Z_t) = \left[\frac{\partial \lambda_t(Z_t)}{\partial t} + \nabla_X \lambda_t(Z_t)^\top V_t - \nabla_V \lambda_t(Z_t)^\top (X_t + 2V_t) + 2\Delta_V \lambda_t(Z_t) \right] dt + 2\nabla_V \lambda_t(Z_t)^\top dW_t,$$

which by plugging in the PDE (86), we end up with

$$d\lambda_t(Z_t) = -2\|\nabla_V \lambda(Z_t, t)\|^2 dt + 2\nabla_V \lambda(Z_t, t)^\top dW_t.$$

It implies the regularizer on the forward control as

$$\text{Var} \left(\lambda(Z_T, T) - \lambda(Z_0, 0) + \int_0^T 2\|\nabla_V \lambda(Z_t, t)\|^2 dt - 2 \int_0^T \nabla_V \lambda(Z_t, t)^\top dW_t \right). \quad (87)$$

Once we have the optimal control $u(Z_t, t)$ from (85), one can simply simulate (79)-(80) from Z_0 to draw samples from μ . We recommend a splitting approach where one alternates between the Hamiltonian part (with reversible symplectic leapfrog denoted by flow map Φ_h), the u_t drift part (with Euler), and the rest OU part (with exact simulation) for SDE discretization.

Backward condition Via a change of variable

$$\log \rho_t(Z_t) = \lambda_t(Z_t) + \eta_t(Z_t), \quad u_t(Z_t) = -\nabla_V \lambda_t(Z_t),$$

now (84) and (86) imply the PDE regularizer on the backward control $o(Z_t, t) = -\nabla_V \eta(Z_t, t)$ should read as

$$\partial_t \eta(Z_t, t) = -\nabla_{[X, V]} \eta(Z_t, t)^\top \bar{b}_t - \nabla \cdot \bar{b}_t + 2\|\nabla_V \eta(Z_t, t)\|^2 + 2\Delta_V \eta(Z_t, t), \quad (88)$$

and the corresponding SDE regularizer along the reference (76)-(77) becomes (using $\nabla \cdot \bar{b}_t = -2d$):

$$d\eta_t(Z_t) = [2\|\nabla_V \eta(Z_t, t)\|^2 + 4\Delta_V \eta(Z_t, t) + 2d] dt + 2\nabla_V \eta(Z_t, t)^\top dW_t.$$

Moreover the boundary condition should match the marginal densities at $t = 0, T$ in the sense that time reversal imposes $u_t(Z_t) + o_t(Z_t) = -\nabla_V \log \rho_t(Z_t)$ for all $t \in [T]$. From (84) the deterministic ODE implementation of the dynamics with given $(u_t(Z_t), o_t(Z_t))$ therefore becomes

$$dZ_t = \begin{bmatrix} dX_t \\ dV_t \end{bmatrix} = \begin{bmatrix} V_t \\ -X_t - 2V_t - 2u_t(Z_t) + 2o_t(Z_t) \end{bmatrix} dt. \quad (89)$$

Remark 17 (Cost and evolution). We would like to note that the reference process (76)-(77) still gives an entropy regularized optimal transport objective with quadratic cost, since

$$\begin{aligned} & \arg \min_{P_0 \sim \nu \otimes \mathcal{N}, P_T \sim \mu \otimes \mathcal{N}} KL(P_{0T} \| Q_{0T}) \\ &= \arg \min_{P_0 \sim \nu \otimes \mathcal{N}, P_T \sim \mu \otimes \mathcal{N}} \mathbb{E}_{P_{0T}} [-\log Q_{T|0}] - \int P(Z_0, Z_T) \log P(Z_0, Z_T) dZ_0 dZ_T \\ &= \arg \min_{P_0 \sim \nu \otimes \mathcal{N}, P_T \sim \mu \otimes \mathcal{N}} \mathbb{E}_{P_{0T}} \left[\underbrace{[(Z_T - M_{0T} Z_0)^\top D_{T|0}^{-1} (Z_T - M_{0T} Z_0)]}_{c_T(Z_0, Z_T)} \right] - H(P_{0T}), \end{aligned} \quad (90)$$

where we used that the conditional distribution of Z_T given Z_0 is Gaussian, which we denote with mean $M_{0T}Z_0$ and covariance $D_{T|0}$. Using the fact that the reference is a linear SDE that admits analytical solution, assuming we initialize as

$$(X_0, V_0) \sim \mathcal{N} \left(\begin{pmatrix} \mu_X^0 \\ \mu_V^0 \end{pmatrix}, \begin{pmatrix} \sigma_{XX}^0 \cdot I & 0 \\ 0 & \sigma_{VV}^0 \cdot I \end{pmatrix} \right),$$

the dynamics will remain Gaussian with

$$\mathbb{E}[Z_T] = \begin{bmatrix} (T+1)\mu_X^0 + T\mu_V^0 \\ -T\mu_X^0 + (1-T)\mu_V^0 \end{bmatrix} e^{-T} = \begin{bmatrix} (T+1)e^{-T} \cdot I & Te^{-T} \cdot I \\ -Te^{-T} \cdot I & (1-T)e^{-T} \cdot I \end{bmatrix} \begin{pmatrix} \mu_X^0 \\ \mu_V^0 \end{pmatrix} \rightarrow 0_{2d}$$

and

$$\text{Cov}[Z_T] = \begin{bmatrix} \sigma_{XX}^T \cdot I & \sigma_{XV}^T \cdot I \\ \sigma_{VX}^T \cdot I & \sigma_{VV}^T \cdot I \end{bmatrix} e^{-2T} \rightarrow \begin{bmatrix} I & 0 \\ 0 & I \end{bmatrix}$$

for

$$\begin{aligned} \sigma_{XX}^T &= (T+1)^2 \sigma_{XX}^0 + T^2 \sigma_{VV}^0 + e^{2T} - 1 - 2T - 2T^2 \\ \sigma_{XV}^T &= \sigma_{VX}^T = -T(T+1) \sigma_{XX}^0 + T(1-T) \sigma_{VV}^0 + 2T^2 \\ \sigma_{VV}^T &= T^2 \sigma_{XX}^0 + (1-T)^2 \sigma_{VV}^0 - 2T^2 + 2T + e^{2T} - 1 \end{aligned}$$

and plugging in $\mu_X^0 = x_0, \mu_V^0 = v_0, \sigma_{XX}^0 = \sigma_{VV}^0 = 0$ gives the desired M_{0T} and $D_{T|0}$. This asymptotic behavior matches our intuition about the equilibrium.

Note that the coupling $P_{0T}(X_0, V_0, X_T, V_T) = \pi^*(X_0, X_T) \mathcal{N}(V_0) \mathcal{N}(V_T)$ for $\int \pi^*(X_0, X_T) dX_T = \nu(X_0)$, $\int \pi^*(X_0, X_T) dX_0 = \mu(X_T)$ is always valid, in which case the objective will simplify to a quadratic involving (X_0, X_T) only since $\mathbb{E}_{P_{0T}}[V_0 V_T] = \mathbb{E}_{P_{0T}}[V_0 X_T] = \mathbb{E}_{P_{0T}}[X_0 V_T] = 0$ and the constraints already enforce $\mathbb{E}_{P_{0T}}[\|V_T\|^2]$ and $\mathbb{E}_{P_{0T}}[\|V_0\|^2]$ to be fixed and $\mathbb{E}_{P_{0T}}[X_T V_T] = \mathbb{E}_{P_{0T}}[X_0 V_0] = 0$. Similarly the entropy term $H(\cdot)$ will also only involve (X_0, X_T) in this case. But generally the marginal over (X_0, X_T) from solving the optimal transport SB problem (90) will not correspond to $\pi^*(X_0, X_T)$ from (27), as we show below.

Lemma 5 (Structure of the joint optimal coupling). *The joint coupling from (90) in general do not factorize over the X and V variables, unless $T \rightarrow \infty$, in which case the coupling over the X variables will favor the independent one, i.e., $\nu(X_0) \otimes \mu(X_T)$.*

Proof. The optimal regularized coupling always takes the form for some f, g

$$\begin{aligned} \pi^*(Z_0, Z_T) &= e^{f(Z_0)} \cdot e^{g(Z_T)} \cdot Q(Z_T|Z_0) \cdot \nu(X_0) \otimes \mathcal{N}(V_0) \otimes \mu(X_T) \otimes \mathcal{N}(V_T) \\ &= e^{f_1(X_0) + f_2(V_0)} \cdot e^{g_1(X_T) + g_2(V_T)} \cdot Q(Z_T|Z_0) \cdot \nu(X_0) \otimes \mu(X_T) \otimes \mathcal{N}(V_0) \otimes \mathcal{N}(V_T) \\ &= [e^{f_1(X_0) + g_1(X_T)} \nu(X_0) \otimes \mu(X_T)] \cdot [e^{f_2(V_0) + g_2(V_T)} \mathcal{N}(V_0) \otimes \mathcal{N}(V_T)] \cdot Q(Z_T|Z_0). \end{aligned}$$

While the rest of the terms may factorize, there will be cross terms between e.g., $X_T - V_0$ and $V_T - X_0$ coming from $Q(Z_T|Z_0)$ unless $T \rightarrow \infty$. Although the cost $\mathcal{C}_T(Z_0, Z_T)$ is still quadratic, since it approaches in that limit

$$\min_{X_T \sim \mu, V_T \sim \mathcal{N}} \mathbb{E}[\|X_T\|^2 + \|V_T\|^2]$$

using Remark 17, which is fixed by the constraint, the second entropy term will dominate and therefore the resulting optimal coupling will be the product distribution. \square

Remark 18 (Gaussian entropy regularized \mathcal{W}_2 transport). In the more commonly studied case when the cost is simply $\|Z_T - Z_0\|^2$, and if both ν and μ are Gaussian with arbitrary covariance, using closed-form expression from (Janati et al., 2020, Theorem 1) we have that the regularized optimal transport plan is Gaussian over $\mathbb{R}^{2d} \times \mathbb{R}^{2d}$:

$$\pi^* \sim \mathcal{N} \left(\begin{pmatrix} [\bar{\nu}, 0]^\top \\ [\bar{\mu}, 0]^\top \end{pmatrix}, \begin{pmatrix} A & C_T \\ C_T^\top & B \end{pmatrix} \right)$$

for

$$A = \begin{bmatrix} \Sigma_\nu & 0 \\ 0 & I \end{bmatrix} \quad B = \begin{bmatrix} \Sigma_\mu & 0 \\ 0 & I \end{bmatrix} \quad C_T = \frac{1}{2} A^{1/2} (4A^{1/2} B A^{1/2} + T^2 I)^{1/2} A^{-1/2} - \frac{T}{2} I.$$

We recognize

$$\frac{1}{2}A^{1/2}(4A^{1/2}BA^{1/2} + T^2I)^{1/2}A^{-1/2} = A^{1/2}(A^{1/2}BA^{1/2} + T^2/4 \cdot I)^{1/2}A^{-1/2} = (AB + T^2/4 \cdot I)^{1/2}$$

as the unique square root of $AB + T^2/4 \cdot I$ with non-negative eigenvalues when $A \succ 0$. Therefore in this case, the optimal entropy-regularized coupling does take the form of $P_{0T}^*(X_0, V_0, X_T, V_T) = \pi^*(X_0, X_T)\bar{\pi}^*(V_0, V_T)$ where π^* and $\bar{\pi}^*$ are respectively the entropy-regularized optimal coupling between the X -variables and the V -variables (i.e., the structure of C_T implies that X and V are uncorrelated).

Normalizing constant estimator Importance-weighted Z -estimators can be derived from the controlled sampling trajectory (79)-(80) using similar ideas as those in Lemma 1 by leveraging the likelihood ratio (83). One can check that the discretized Z estimator can be written as

$$\begin{aligned} & \frac{1}{N} \sum_{i=1}^N \exp \left(\log \frac{\mu(X_K) \otimes \mathcal{N}(V_K)}{\nu(X_0) \otimes \mathcal{N}(V_0)} + \right. \\ & \left. \sum_{k=0}^{K-1} \frac{1}{2(1 - e^{-2h})} \|\hat{V}_{k+1}^i - e^{-h}V_k^i\|^2 - \frac{1}{2(1 - e^{-2h})} \|V_k^i - e^{-h}\{\Phi_{-h}(Z_{k+1}^i)\}_V + 4h\nabla_V \eta_{k+1}(\Phi_{-h}(Z_{k+1}^i))\|^2 \right) \end{aligned} \quad (91)$$

for 3-stage splitting updates

$$\hat{V}_{k+1} \sim \mathcal{N}(e^{-h}V_k, (1 - e^{-2h})I), \tilde{V}_{k+1} = \hat{V}_{k+1} + 4h \cdot \nabla_V \lambda_k(X_k, \hat{V}_{k+1}), Z_{k+1} = (X_{k+1}, V_{k+1}) = \Phi_h(X_k, \tilde{V}_{k+1})$$

from $Z_0 \sim \nu \otimes \mathcal{N}(0, I)$. Notice the last two parts are purely deterministic and the first two parts act solely on the variable V , which explains the last line in (91).

G ADDITIONAL NUMERICAL EXPERIMENTS

We provide additional details on the numerical experiments in this section. Compared to MCMC, our method is gradient free and since it takes a more global perspective on the path space, it can be less susceptible to mode collapse and/or long escape time. This type of path-based sampler also comes with importance weighting correction and has normalizing constant estimator built in as an output.

G.1 Benchmark and Metrics

The following 4 targets are considered with different priors ν :

- 2D standard Gaussian: $\mathcal{N}(x; 0, I)$ with prior $\nu(x) = \mathcal{N}(x; 0, 2I)$
- Funnel: $x_0 \sim \mathcal{N}(0, 3^2), x_1|x_0 \sim \mathcal{N}(0, \exp(x_0))$ with prior $\nu(x) = \mathcal{N}(x; 0, 2I)$
- Gaussian mixture model with 9 modes: $\frac{1}{9} \sum_{i=1}^9 \mathcal{N}(x; \mu_i, I)$ where $\{\mu_i\}_{i=1}^9 = \{-5, 0, 5\} \times \{-5, 0, 5\}$ with prior $\nu(x) = \mathcal{N}(x; 0, 3.5^2 I)$
- Double well: $\mu(x) \propto -(x_0^2 - 2)^2 - (x_1^2 - 2)^2$ with prior $\nu(x) = \mathcal{N}(0, 2I)$

For each of the benchmarks and 4 losses, we plot the marginals and report the following:

- Absolute error in mean and relative error in standard deviation compared to the ground truth using importance-weighted Monte-Carlo estimates (93)
- The log normalizing constant $\log Z$ estimator (c.f. Lemma 1):

$$\log \left(\frac{1}{n} \sum_{i=1}^n \frac{\mu(x_{K+1}^i)}{\nu(x_0^i)} \exp \left[\sum_{k=0}^K \frac{1}{2} \|Z_k^i\|^2 - \sum_{k=0}^K \frac{1}{2\sigma^2 h} \|x_k^i - x_{k+1}^i - \sigma^2 h \nabla \psi(x_{k+1}^i, (k+1)h)\|^2 \right] \right)$$

using the final trajectory $\{x_k^i\}$ from (18).

Importance weighting For the very last sampling SDE, we simulate (18) with the latest $\nabla \phi$, but re-weight the n samples $\{x_{K+1}^i\}_{i=1}^n$ each with individual (un-normalized) weight

$$w^\phi(x_{K+1}^i) = \frac{\mu(x_{K+1}^i)}{\nu(x_0^i)} \exp \left(h \left[\sum_{k=0}^K \frac{\sigma^2}{2} \Delta \phi(x_k^i, kh) - \frac{\sigma^2}{2} \Delta \psi(x_k^i, kh) \right] \right) \quad (92)$$

before taking their average, i.e.,

$$\hat{\mathbb{E}}_{p_{\text{target}}} [g] = \frac{\sum_{i=1}^n g(x_{K+1}^i) w^\phi(x_{K+1}^i)}{\sum_{i=1}^n w^\phi(x_{K+1}^i)} \quad (93)$$

for a summary statistics $g : \mathbb{R}^d \rightarrow \mathbb{R}$ we are interested in. This estimator follows from Proposition 2 and is used for post-processing with a potentially suboptimal control $\nabla \phi$, caused by e.g., approximation or optimization error from neural network training.

G.2 Result

For the experiments, we parameterize $\phi, \psi : \mathbb{R}^d \times [0, c] \rightarrow \mathbb{R}$ as residual feed-forward neural networks where c is a hyperparameter. Each network first maps the input vector to a hidden state with a linear transformation, which is then propagated through several residual layers that maintain hidden state dimensionality. Each residual layer receives as input a state-time pair $(x, t) \in \mathbb{R}^{d+1}$ and outputs $\sigma(W(x, t) + b) + x$, where σ is the ReLU activation function. The number of hidden layers and their sizes vary by target distribution. Adam optimizer was used to train the models with $\beta_1 = 0.9, \beta_2 = 0.999$, and weight decay 0.01, where batches of trajectories are used for several steps of gradient updates in each epoch, before regenerating the n trajectories and estimating the objective for the next round of updates on the NN parameters. Across all experiments, we initialize $\phi(x_0^i, 0) \approx \log \mu(x_0^i)$. For fair comparison, the training process is stopped when the loss stops noticeably decreasing.

For a comparison on the computation speed of the four regularizers: for the standard normal target it took 624 seconds to train with PINN, 108 seconds with the Variance regularizer, 106 seconds with TD, and 85 seconds with Separate Control. Generating trajectories requires much less time than evaluating the loss and its gradient. Computing each loss requires processing all K states across n trajectories. Combined with the number of training epochs and the number of updates per batch, we estimate the processing time per trajectory state as approximately

$$\frac{\text{training_time}}{\text{epochs} \times \text{trajectories} \times \text{updates_per_batch} \times K}$$

The stated processing time is therefore roughly $6.2 \cdot 10^{-3}$ s for PINN, $3.6 \cdot 10^{-7}$ s for Variance, $3.5 \cdot 10^{-7}$ s for TD, and $2.8 \cdot 10^{-7}$ s for Separate Control. The latter three are comparable and much faster than PINN whose Laplacian computation adds an order of magnitude processing time. This efficiency comparison is also independent of the target distribution.

For reproducibility, the anonymous Github repository can be found at the following link:

<https://anonymous.4open.science/r/diffusion-sampler-E4F7>

where hyperparameters used for the experiments are listed in the corresponding notebooks.

In Table 2, Table 3 and Figure 3, Figure 4, Figure 5 below we present the simulation results. All experiments are run with a GeForce RTX 2080 GPU and an AMD Ryzen 9 3900X CPU.

	PINN	Variance	TD	Separate control
Standard normal	0.232	0.382	0.241	0.221
Funnel	0.795	0.797	0.795	0.811
GMM	0.172	0.088	0.134	0.033
Double well	0.161	0.178	0.008	0.026

Table 2: Relative error of weighted empirical standard deviation (lower is better)

	PINN	Variance	TD	Separate control
Standard normal	0.124	0.038	0.014	0.031
Funnel	0.787	0.296	0.255	0.155
GMM	0.632	0.039	0.289	0.301
Double well	0.234	0.736	0.166	0.362

Table 3: Absolute error of empirical mean (lower is better)

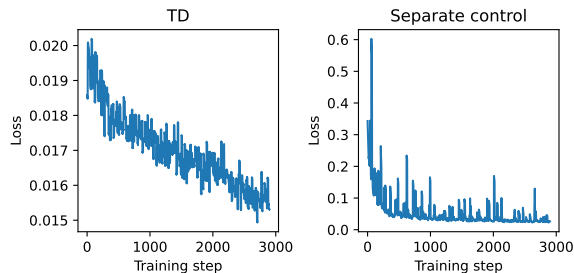


Figure 3: Training loss plot for GMM with TD and Separate Control

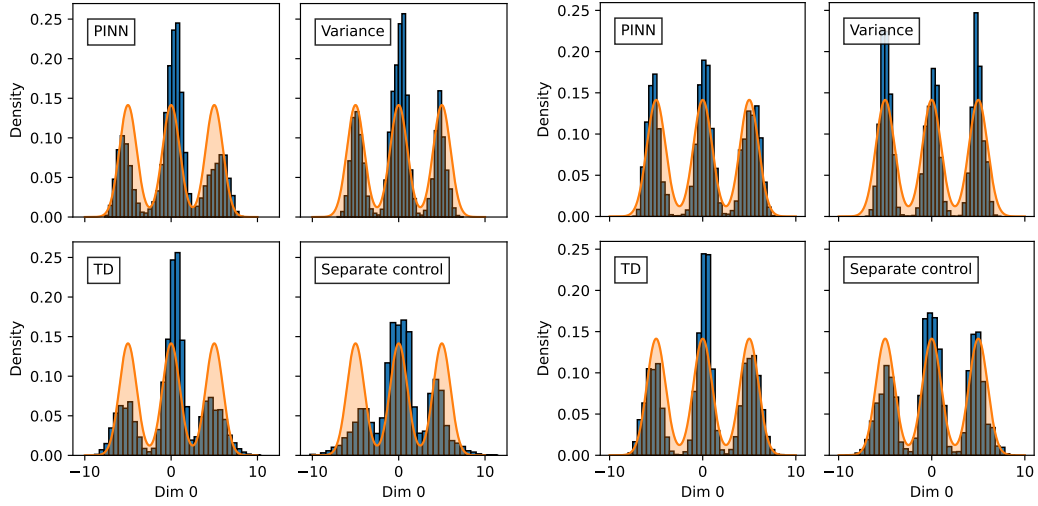


Figure 4: GMM marginal before (left) and after (right) importance weighting

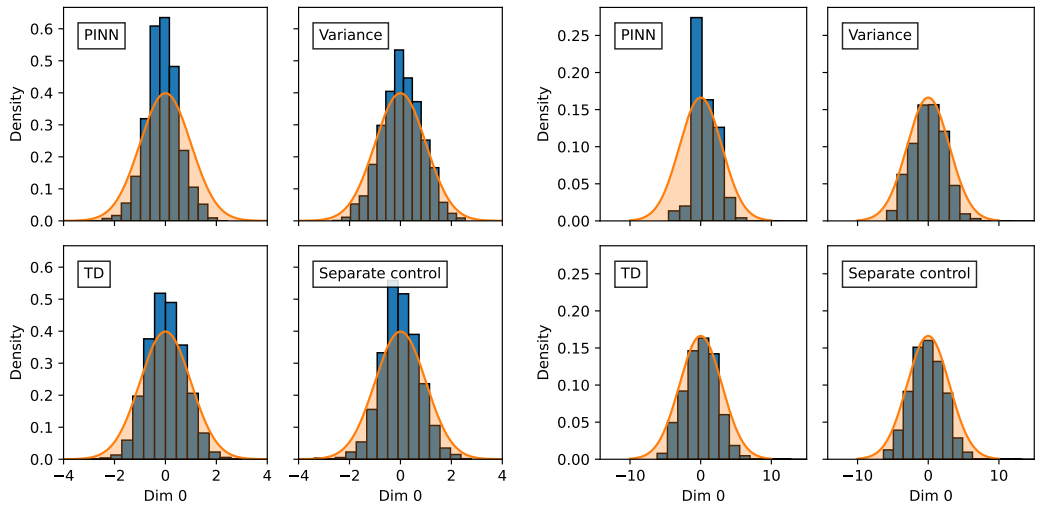


Figure 5: Standard normal marginal (left) and Funnel marginal (right) with importance weighting

G.3 Application in Optimal Transport and Stochastic Control

In contrast to (Chen et al., 2021a), we are guaranteed optimal control in the sense of SB, beyond just terminal marginal constraint matching. In this regard, the two works target different purposes (i.e., trajectories), and we illustrate these optimal transport and control benefits in Table 4.

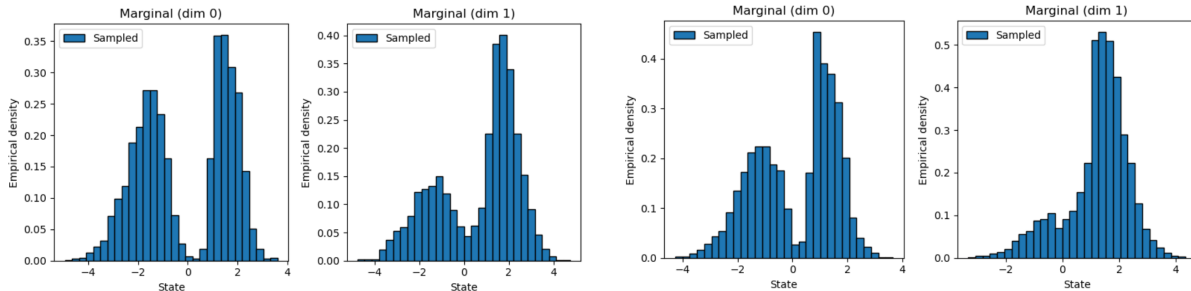


Figure 6: Double-well experiment: marginal distribution (non importance-weighted) from our variance-regularized loss (22) on the left vs. method in (Chen et al., 2021a) without regularization on the right. Absolute error in mean: 0.31 (ours) vs. 0.35 (Chen et al., 2021a).

Algorithm	Entropy-regularized \mathcal{W}_2 distance	Control Cost $\mathbb{E}_{X \sim \mathbb{P}^{\nu, \sigma^2 \nabla \phi}} [\int_0^T \frac{\sigma^2}{2} \ \nabla \phi_t(X_t)\ ^2 dt]$
Ours	1.94	1.62
Method of (Chen et al., 2021a)	2.50	2.31

Table 4: Comparison of (Chen et al., 2021a) vs. our SB method (22) on double-well experiment: both are two-parameter losses but ours aim at identifying the *unique optimal control* when setting the regularization parameter $\lambda > 0$. We observe that our method preserves marginals with a better bridge interpolation and less control energy spent ($T = 1$ is picked in all experiments).

Dimension (Method)	Entropy-regularized \mathcal{W}_2 distance	Absolute error in mean estimator
2 (ours)	1.94	0.31
2 (DDS (Vargas et al., 2022))	2.28	0.39

Table 5: Comparison of eqn (9) in DDS (Vargas et al., 2022) as one-parameter loss vs. our SB two-parameter loss (22). We observe (1) better trajectory property in the sense of optimal transport; (2) one requires slightly larger network size for method (Vargas et al., 2022) to give satisfying results.